Articles

Synthetic and Mechanistic Studies of the Four-Electron Reduction of Dioxygen, N═N, and N═O Double Bonds by Tungsten(II) Aryloxide Compounds

Margaret R. Lentz, Jonathan S. Vilardo, Mark A. Lockwood, Phillip E. Fanwick, and Ian P. Rothwell*

Department of Chemistry, Purdue University, 560 Oval Drive, West Lafayette, Indiana 47907-2038

Received September 16, 2003

Reduction of the cyclometalation-resistant aryloxide compounds [W(OC_6HPh_2-2,6-R_2-3,5)$_2$-Cl_4] (**1**, R = Ph; **2**, R = Me; **3**, R = Bu^t) in the presence of a variety of phosphine ligands generates the W(II) species [W(OC_6HR_2Ph-η^6-C_6H_4)(OC_6HPh_2-2,6-R_2-3,5)(L)] (**4**−**6**) in moderate yield. Compounds **4**−**6** contain a three-legged piano-stool geometry with one of the aryloxide ligands chelated to the tungsten via an ortho phenyl ring. Solid-state structural parameters for the PMe_3, PEt_3, and PBu^n_3 adducts **4b**−**d** indicate a shortening of the W−C(ipso) and W−C(para) distances consistent with a tungstanorbornadiene resonance contribution. Solution studies of **4b** show that exchange on the NMR time scale of ortho and meta protons occurs at elevated temperatures via phosphine dissociation and not π-arene dissociation. Reaction of **4b** with O_2 or the *trans*-diazines PhN═NPh, TolN═NTol, and PhN═NTol (Tol = 4-methylphenyl) led to the corresponding bis(oxo) and bis(arylimido) derivatives [W(OC_6HPh_4-2,3,5,6)$_2$(X)$_2$(PMe_3)] (X = O, NPh, Ntol; **7**−**10**, respectively). Structural studies show a trigonal-bipyramidal geometry for **7** and **10** with equatorial O or NAr groups and an axial PMe_3. Formation of the mixed-imido species [W(OC_6HPh_4-2,3,5,6)$_2$(NPh)(NTol)(PMe_3)] (**10**) did not involve generation of any **8** or **9**. Cleavage of nitrosobenzene by **4b** led to [W(OC_6-HPh_4-2,3,5,6)$_2$(NPh)(O)($OPMe_3$)] (**11**) containing terminal oxo and phenylimido groups and a phosphine oxide donor ligand. Compound **4b** was also found to ring-open the substrates pyridazine, benzo[*c*]cinnoline, and phthalazine to produce the three new seven-membered diaza metallacycles **12**−**14**. Structural studies show **12** and **14** to contain planar rings, whereas the two backbone phenyl rings in **13** are twisted by 33° with respect to each other. Structural parameters are more consistent with a formulation as a d^0-W(VI) metal center with a 2,7-diazatungstahepta-1,3,5,7-tetraene ring and two tungsten−imido bonds for **12** and **14**, although there is some evidence for a 2,7-diazatungstahepta-2,4,6-triene (d^2-W(IV) metal center) resonance contribution for **14**. A kinetic study of the reaction of **4b** with *trans*-4,4′-dimethylazobenzene (TolN═NTol) to produce **9** was carried out. The rate of disappearance of **4b** was monitored using ^{1}H NMR and shown to have a first-order dependence on both [**4b**] and [TolN═NTol] and inverse first-order dependence on [PMe_3]. The kinetic data was fit to a mechanistic model involving fast exchange of azobenzene with PMe_3 followed by a rate-determining product formation. The concentration of free PMe_3 (strong inhibition) is controlled by the position of the fast coordination equilibrium of the product [W(OC_6HPh_4-2,3,5,6)$_2$(NTol)$_2$(PMe_3)] (**9**). Reaction of *trans*-MesN═NMes (NMes = $NC_6H_3Me_3$-2,4,6) with **4b** was slow even at 100 °C. However, photolysis to produce *cis*-MesN═NMes led to rapid room-temperature formation of [W(OC_6HPh_4-2,3,5,6)$_2$(NMes)$_2$] (**15**). The many orders of magnitude rate acceleration for *cis*-diazines over their trans counterparts combined with all the other mechanistic work makes a compelling argument that these cleavage reactions (four-electron reductions) are taking place at a single metal center.

Introduction

There continues to be a great deal of interest in the inorganic and organometallic chemistry associated with monoanionic alkoxide,[1,2] aryloxide, siloxide,[2] and amido[3] ligation. With the group 4−6 metals, these π-donating ligands have a tendency to stabilize the metals in their highest formal oxidation states (d^0 electron configura-

* To whom correspondence should be addressed. E-mail: rothwell@purdue.edu.

(1) Bradley, D. C.; Mehrotra, R. C.; Rothwell, I. P.; Singh, A. *Alkoxo and Aryloxo Derivatives of Metals*; Academic Press: San Diego, CA, 2001.

(2) (a) Wolczanski, P. T. *Polyhedron* **1995**, *14*, 3335. (b) Marciniec, B.; Maciejewski, H. *Coord. Chem. Rev.* **2001**, *223* 301. (c) Chisholm, M. H. *Chemtracts: Inorg. Chem.* **1992**, *4*, 273.

10.1021/om030604m CCC: $27.50
Publication on Web 01/07/2004

Scheme 1

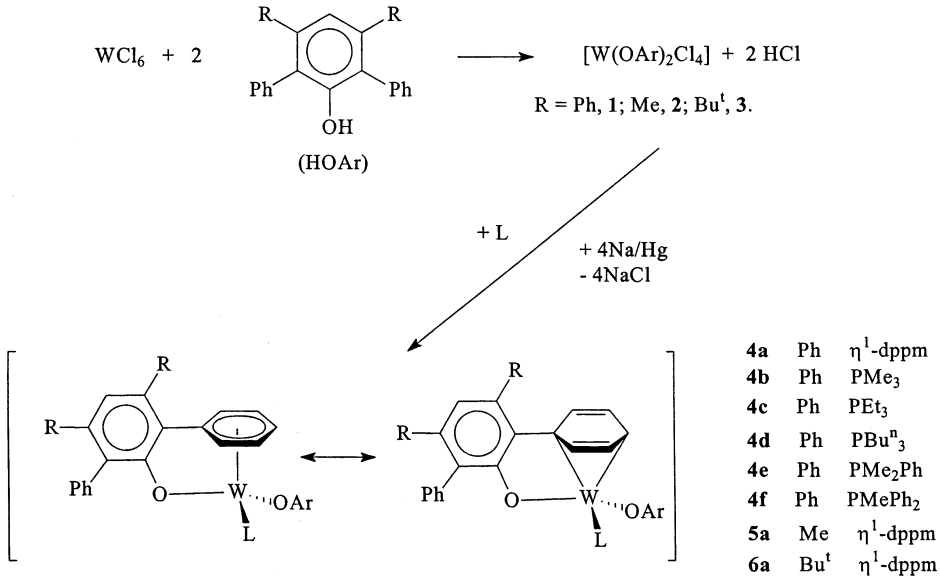

tion). With small ligation the lower redox states tend to be dominated by dinuclear compounds containing metal−metal bonds of various bond orders.[4] Mononuclear species can be stabilized either by electronically saturating the coordination sphere or by the use of bulky ligation.[5] In the latter case the resulting low-coordinate compounds can exhibit reactivity involving the binding and reduction of important substrates, including dinitrogen.

In the case of early d-block metal aryloxide chemistry, our group and others have found that 2,6-disubstituted phenoxides have a nagging tendency to undergo facile intramolecular CH bond activation at low-valent metal centers.[6,7] Recently we have demonstrated the inhibition of cyclometalation processes with 2,6-diphenylphenoxide ligands by the introduction of meta substituents onto the phenoxide nucleus.[8] In this paper we report on the use of these "cyclometalation resistant" ligands to stabilize low-valent, mononuclear derivatives of tungsten. The exploitation of these species for the four-electron reduction of important substrates such as dioxygen, organic diazo, and nitroso compounds is reported.[9,10] Particular emphasis is placed on the mechanistic aspects of the cleavage of the N=N bond in cis/trans diazo compounds and the possible reaction pathways. We have previously communicated some aspects of this work as well as a thorough theoretical analysis of the reactivity of *cis*-diazines with these tungsten reagents.[11,12] A very recent publication has dealt with related low-valent tungsten aryloxides containing pyridine ligation.[13]

Results and Discussion

Synthesis and Solid-State Structure of W(II) Aryloxides. Previous studies have shown that the sodium amalgam reduction of the tetrachloride species $[W(OC_6H_3Ph_2\text{-}2,6)_2Cl_4]$, in the presence of phosphine ligands (L), typically leads to the bis-cyclometalated compounds $[W(OC_6H_3Ph\text{-}\eta^1\text{-}C_6H_4)_2(L)_2]$ (**I**). With the choice of a suitable phosphine, the deep green compound $[W(OC_6H_3Ph\text{-}\eta^6\text{-}C_6H_5)(OC_6H_3Ph_2\text{-}2,6)(L)]$ (**II**) can also be isolated and shown to thermally convert to the cyclometalated species and H_2.[12b]

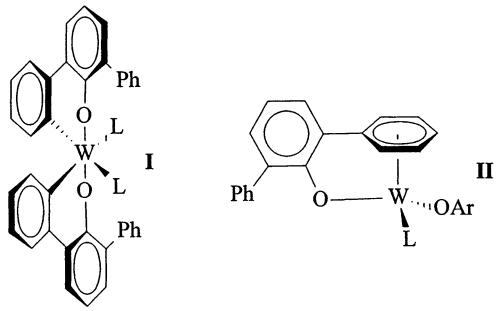

(3) (a) Gade, L. H. *Acc. Chem. Res.* **2002**, *35*, 575. (b) Fryzuk, M. D. In *Modern Coordination Chemistry*; Leigh, G. J., Winterton, N., Eds.; Royal Society of Chemistry: Cambridge, U.K., 2002; pp 187−207. (c) Kempe, R.; Noss, H.; Irrgang, T. *J. Organomet. Chem.* **2002**, *647*, 12. (d) Holland, P. L.; Andersen, R. A.; Bergman, R. G. *Comments Inorg. Chem.* **1999**, *21*, 115. (e) Schrock, R. R. *Acc. Chem. Res.* **1997**, *30*, 9. (f) Beswick, M. A.; Wright, D. S. *Coord. Chem. Rev.* **1998**, *176*, 373.

(4) Cotton, F. A.; Walton, R. A. *Multiple Bonds Between Metal Atoms*, 2nd ed.; Wiley: New York, 1998.

(5) Cummins, C. C. *Prog. Inorg. Chem.* **1998**, *47*, 685.

(6) (a) Rothwell, I. P. *Acc. Chem. Res.* **1988**, *21*, 153. (b) Lefebvre, F.; Leconte, M.; Pagano, S.; Mutch, A.; Basset, J.-M. *Polyhedron* **1995**, *14*, 3209. (c) Chesnut, R. W.; Durfee, L. D.; Fanwick, P. E.; Rothwell, I. P.; Folting, K.; Huffman, J. C. *Polyhedron* **1987**, *6*, 2019.

(7) The cyclometalation of a variety of aryloxide ligands by low-valent Mo, W systems has been demonstrated; see: (a) Hascall, T.; Murphy, V. J.; Janak, K. E.; Parkin, G, *J. Organomet. Chem.* **2002**, *652*, 37. (b) Hascall, T.; Baik, M. H.; Bridgewater, B. A.; Shin, J. H.; Churchill, D. G.; Friesner, R. A.; Parkin, G. *Chem. Commun.* **2002**, 2644. (c) Rabinovich, D.; Zelman, R.; Parkin, G. *J. Am. Chem. Soc.* **1990**, *112*, 9632. (d) Rabinovich, D.; Zelman, R.; Parkin, G. *J. Am. Chem. Soc.* **1992**, *114*, 4611.

(8) (a) Vilardo, J. S.; Lockwood, M. A.; Hanson, L. G.; Clark, J. R.; Parking, B. C.; Fanwick, P. E.; Rothwell, I. P. *J. Chem. Soc., Dalton Trans.* **1997**, 3353. (b) Lockwood, M. A.; Clark, J. R.; Parkin, B. C.; Rothwell, I. P. *J. Chem. Soc., Chem. Commun.* **1996**, 1973. (c) Lockwood, M. A.; Potyen, M. C.; Steffey, B. D.; Fanwick, P. E.; Rothwell, I. P. *Polyhedron* **1995**, *14*, 3293.

(9) For the pioneering use of W(II) halides for the cleavage of C=N and C=O bonds see: Bryan, J. C.; Mayer, J. M. *J. Am. Chem. Soc.* **1990**, *112*, 2298.

(10) For cleavage of ketones by ditungsten systems see: (a) Chisholm, M. H.; Folting, K.; Klang, J. A. *Organometallics* **1990**, *9*, 602. (b) Chisholm, M. H.; Folting, K.; Klang, J. A. *Organometallics* **1990**, *9*, 607.

(11) Maseras, F.; Lockwood, M. A.; Eisenstein, O.; Rothwell, I. P. *J. Am. Chem. Soc.* **1998**, *120*, 6598.

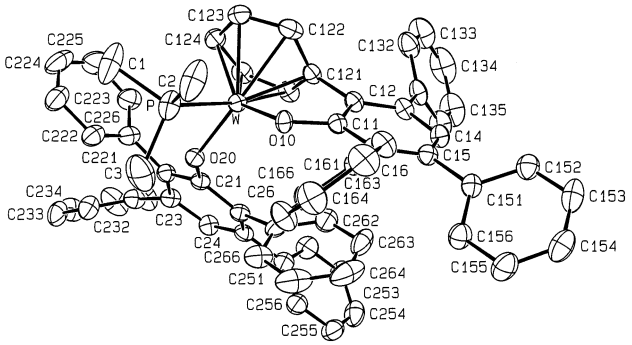

Figure 1. Molecular structure of $[W(OC_6HPh_3\text{-}\eta^6\text{-}C_6H_5)(OC_6HPh_4\text{-}2,3,5,6)(PMe_3)]$ (**4b**).

In contrast, reduction of the meta-substituted compounds $[W(OC_6HPh_2\text{-}2,6\text{-}R_2\text{-}3,5)_2Cl_4]$ (**1**, R = Ph; **2**, R = Me; **3**, R = Bu^t) in the presence of a variety of phosphine ligands generates the W(II) species $[W(OC_6HR_2Ph\text{-}\eta^6\text{-}C_6H_5)(OC_6HPh_2\text{-}2,6\text{-}R_2\text{-}3,5)(L)]$ (**4**−**6**) in moderate yield (Scheme 1). Solutions of these deep green compounds in C_6D_6 are unchanged (NMR) after being heated at 100 °C for hours. The molecular structures of these compounds are of particular interest. A related pyridine adduct has also been recently reported.[13] Four derivatives, **4b**−**e**, have been subjected to single-crystal X-ray diffraction analysis. An ORTEP view of the PMe_3 derivative **4b** is shown in Figure 1, and a comparison of key structural parameters is given in Table 1. The compounds all adopt a three-legged piano-stool geometry with one of the aryloxide ligands chelated to the tungsten via an η^6-arene interaction through an ortho phenyl ring. The chelated aryloxide has a W−O−Ar angle of 118−119°, which is slightly smaller than that of the terminal ligand (126−134°), and also has a slightly elongated W−O bond length. However, neither the W−O nor W−P distances appear to be sensitive to the nature of the phosphine ligand. Of most interest are the structural parameters for the W−η^6-arene interaction. There are a large number of structurally characterized tungsten compounds that contain an η^6-arene ligand. Ubiquitous examples are the $[W(arene)_2]$ and $[(arene)W(CO)_3]$ 18-electron series. Analysis of typical W−C(arene) distances for representative compounds of this type show a narrow range of values: cf. 2.25(2)−2.32(2) Å for $[W(\eta^6\text{-}C_6H_5Me)_2]$,[14] 2.244(8)−2.28(1) Å for $[W(\eta^6\text{-}C_6F_6)_2]$,[15] 2.353(5)−2.375(5) Å for $[(\eta^6\text{-}C_6H_6)W(CO)_3]$,[16] and 2.32(2)−2.37(2) Å for $[(\eta^6\text{-}C_6H_3Me_3)W(CO)_3]$.[17] The W−C(arene) distances for **4b**−**e** (Table 1) are more dissimilar. It can be seen that the W−C{ipso, C(121)} carbon distance is short, ranging from 2.16(1) to 2.189(5) Å for the series. This distance is very close to that reported for discrete tungsten−aryl σ bonds: cf. 2.096(5)−2.199(5) Å in $[W(O)(C_6H_2Me_3\text{-}2,4,6)_3(THF)]$,[18] 2.18(2) Å in $[W(OC_6H_3Ph\text{-}C_6H_4)_2(PMePh_2)_2]$,[19] 2.155(6) Å in $[Cp^*W(O)(NC_6H_4Me\text{-}4)(C_6H_4Me\text{-}2)]$,[20] 2.203(6) Å in $[W(O)_2(Ph)_2(bipy)]$,[21] 2.14(3) and 2.10(3) Å in $[W_2(OPr^i)_4(C_6H_4Me\text{-}4)_2(HNMe_2)]$,[22] and 2.120(5) and 2.160(5) Å in $[Cp^*W(NO)(C_6H_4Me\text{-}2)_2]$.[23] It can also be seen that the W−C{para, C(124)} distance is also shorter, 2.18(1)−2.228(5) Å, than the remaining W−C{ortho, C(122) and C(126; meta, C(123) and C(125)} distances (Table 1). This particular type of distortion of π-bound arene rings has been observed in other early d-block metal systems.[24] This is not to be confused with the situation where arene rings interact through part or all of the ring carbons with high-valent, electron-deficient d^0-metal centers.[25,26] Instead, the more dramatic distortion is sometimes observed when the arene is bound to a

Table 1. Selected Bond Distances (Å) and Angles (deg) for $[W(OC_6HPh_3\text{-}\eta^6\text{-}C_6H_5)(OC_6HPh_4\text{-}2,3,5,6)(L)]$

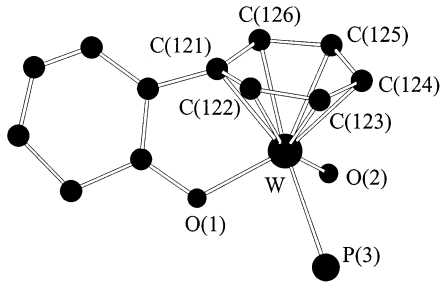

	L			
	PMe_3 (**4b**)	PEt_3 (**4c**)	PBu^n_3 (**4d**)	PMe_2Ph (**4e**)
W−O(1)	2.028(3)	2.014(3)	2.025(4)	2.022(9)
W−O(2)	1.990(3)	1.985(3)	1.987(4)	1.966(9)
W−C(121)	2.171(4)	2.189(5)	2.164(6)	2.16(1)
W−C(122)	2.335(4)	2.332(5)	2.343(7)	2.35(1)
W−C(123)	2.267(4)	2.281(5)	2.285(6)	2.25(1)
W−C(124)	2.201(4)	2.228(5)	2.212(7)	2.18(1)
W−C(125)	2.277(4)	2.284(5)	2.272(7)	2.27(1)
W−C(126)	2.277(4)	2.291(5)	2.256(7)	2.24(2)
W−P(3)	2.474(1)	2.495(1)	2.492(2)	2.478(4)
C(121)−C(122)	1.440(6)	1.452(7)	1.455(9)	1.41(2)
C(122)−C(123)	1.396(6)	1.402(7)	1.365(9)	1.39(2)
C(123)−C(124)	1.439(7)	1.431(7)	1.446(9)	1.43(2)
C(124)−C(125)	1.424(7)	1.424(8)	1.417(9)	1.44(2)
C(125)−C(126)	1.417(6)	1.411(7)	1.398(9)	1.36(2)
C(126)−C(121)	1.439(6)	1.440(7)	1.433(8)	1.46(2)
P(3)−W−O(1)	78.58(8)	79.6(1)	82.0(1)	80.2(3)
P(3)−W−O(2)	82.99(9)	85.9(1)	83.4(1)	85.6(3)
O(1)−W−O(2)	116.3(1)	112.2(1)	114.1(2)	115.3(8)
W−O(1)−C(11)	118.4(2)	119.3(3)	118.4(4)	119.5(8)
W−O(2)−C(21)	130.2(3)	126.2(3)	133.9(4)	130.8(9)

(12) (a) Lockwood, M. A.; Fanwick, P. E.; Eisenstein, O.; Rothwell, I. P. *J. Am. Chem. Soc.* **1996**, *118*, 2762. (b) Kerschner, J. L.; Rothwell, I. P.; Huffman, J. C.; Streib, W. E. *Organometallics* **1988**, *7*, 1871. (c) Lockwood, M. A.; Fanwick, P. E.; Rothwell, I. P. *J. Chem. Soc., Chem. Commun.* **1996**, 2013. (d) Lentz, M. R.; Fanwick, P. E.; Rothwell, I. P. *Chem. Commun.* **2002**, 2482. (e) Lockwood, M. A.;. Fanwick, P. E.; Rothwell, I. P. *Organometallics* **1997**, *16*, 3574.

(13) (a) Lentz, M. R.; Fanwick, P. E.; Rothwell, I. P. *Organometallics* **2003**, *22*, 2259. (b) See also: Kriley, C. E.; Fanwick, P. E.; Rothwell, I. P. *J. Am. Chem. Soc.* **1994**, *116*, 5225.

(14) Prout, K.; Gourdon, A.; Couldwell, C.; Meunier, B.; Miao, F. M.; Woolcock, J. *Acta Crystallogr., Sect. B* **1982**, *38*, 456.

(15) Barker, J. J.; Orpen, A. G.; Seeley, A. J.; Timms, P. L. *J. Chem. Soc., Dalton Trans.* **1993**, 3097.

(16) Oh, J. M.; Geib, S. J.; Cooper, N. J. *Acta Crystallogr., Sect. C: Cryst. Struct. Commun.* **1998**, *54*, 581.

(17) Calderazzo, F.; Poli, R.; Barbati, A.; Zanazzi, P. F. *J. Chem. Soc., Dalton Trans.* **1984**, 1059.

(18) Seidel, W.; Kirsten, G.; Gorls, H. *Z. Anorg. Allg. Chem.* **1998**, *624*, 887.

(19) Kerschner, J. L.; Rothwell, I. P.; Huffman, J. C.; Streib, W. E. *Organometallics* **1988**, *7*, 1871.

(20) Legzdins, P.; Rettig, S. J.; Ross, K. J.; Veltheer, J. E. *J. Am. Chem. Soc.* **1991**, *113*, 4361.

(21) Zhang, C.; Zhang, X.; Liu, N. H.; Schrauzer, G. N.; Schlemper, E. O. *Organometallics* **1990**, *9*, 1307.

(22) Chisholm, M. H.; Eichhorn, B. W.; Folting, K.; Huffman, J. C.; Tatz, R. J. *Organometallics* **1986**, *5*, 1599.

(23) Legzdins, P.; Rettig, S. J.; Ross, K. J.; Batchelor, R. J.; Einstein, F. W. B. *Organometallics* **1995**, *14*, 5579.

(24) (a) Neithamer, D. R.; Parkanyi, L.; Mitchell, J. F.; Wolczanski, P. T. *J. Am. Chem. Soc.* **1988**, *110*, 4421. (b) Veige, A. S.; Kleckley, T. S.; Chamberlin, R. M.; Neithamer, D. R.; Lee, C. E.; Wolczanski, P. T.; Lobkovsky, E. B.; Glassey, W. V. *J. Organomet. Chem.* **1999**, *591*, 194. (c) Veige, A. S.; Wolczanski, P. T.; Lobkovsky, E. B. *Angew. Chem., Int. Ed.* **2001**, *40*, 3629.

highly reducing metal fragment.[27−29] One thoroughly studied system is the set of tantalum arene compounds isolated by Wigley et al.[30] These compounds are generated via the cyclotrimerization of alkynes at d^2-Ta(III) metal centers containing aryloxide ancillary ligation. A theoretical analysis of the distortion has been carried out, and a bonding description involving a tantalanorbornadiene resonance picture has been proposed.[31] In the case of compounds **4**−**6** the chelated arene is bound to a formally d^4-W(II) metal. It would appear that a tungstanorbornadiene resonance picture is also valid (Scheme 1) in which the arene ring is partially reduced with incipient W−C(σ) bonds to the ipso and para carbons. The shorter C(122)−C(123) and C(125)−C(126) distances within the arene ring are consistent with this picture. The distortion of the arene ring bound in **4b**−**e** and previously isolated 2,6-diphenylphenoxide analogues is highlighted by the "radar" plots in Figure 2. It can also be seen that there is an asymmetry involving elongation of the ortho carbon located trans to the terminal aryloxide oxygen atom (Figure 2). Strong support for the tungstanorbornadiene resonance picture comes from reactivity studies, where it has been shown that ketones and aldehydes will insert directly into the W−C(para) bond.[12]

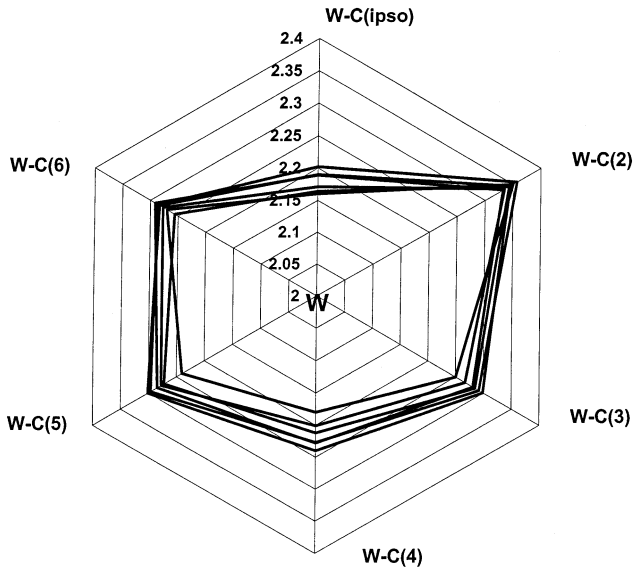

Figure 2. "Radar" plot of the W−C(arene) distances in compounds **4b**−**e**, and [W($OC_6H_3Ph_2$-2,6)(OC_6H_3Ph-η^6-C_6H_5)($PMePh_2$)], and [W($OC_6H_3Ph_2$-2,6)(OC_6H_3Ph-η^6-C_6H_5)-(η^1-dppm)] (solid lines). Also shown is the data for [(η^6-C_6H_6)$W(CO)_3$] (dashed line). The arene coordination is exaggerated by using a plot scale of 2.0−2.4 Å from the metal center.

Spectroscopic Properties and Solution Dynamics of W(II) Aryloxides. Solution studies of these compounds are important, in that they indicate that phosphine dissociation (in the absence of decrease in π-arene interaction) provides the open coordination site for substrate binding. For the compounds **4b**−**f** containing a monodentate phosphine ligand, a sharp resonance is observed in the ^{31}P NMR spectrum with well-resolved ^{183}W satellites. The value of the $^1J(^{183}W-^{31}P)$ coupling constant varies from 362 Hz for the $PMePh_2$ compound **4f** to 372 Hz for the PMe_3 compound **4b**. In the case of the dppm derivatives **4a**, **5a**, and **6a**, two doublets are observed. The resonance in the δ 52−58 ppm region exhibits ^{183}W satellites, $^1J(^{183}W-^{31}P)$ = 342−358 Hz, and can be assigned to the metal-bound phosphorus atom. The second doublet at δ −24 to −25 ppm lies very close to that of free dppm and can be assigned to the uncoordinated, "dangling" phosphorus atom of the monodentate dppm ligand.

At ambient temperatures the ^{1}H NMR spectra of all compounds show the expected phosphine ligand resonances. In the case of compound **4e** the W−PMe_2Ph methyl groups are diastereotopic and appear as two distinct doublets, consistent with the geometry observed in the solid state. A complex multiplet pattern in the aromatic region is observed for all compounds due to the majority of aryloxide protons and any phosphine ligand phenyl ring protons. The π-bound arene ring protons appear considerably upfield of the aromatic region (Figure 3) as five distinct resonances. The lack of a plane of symmetry through the three-legged pianostool geometry results in nonequivalent ortho and meta

(25) (a) Thorn, M. G.; Etheridge, Z. C.; Fanwick, P. E.; Rothwell, I. P. *Organometallics* **1998**, *17*, 3636. (b) Thorn, M. G.; Etheridge, Z. C.; Fanwick, P. E.; Rothwell, I. P. *J. Organomet. Chem.* **1999**, *591*, 148. (c) Pellecchia, C.; Pappalardo, D.; Oliva, L.; Zambelli, A. *J. Am. Chem. Soc.* **1995**, *117*, 6593. (d) Pellecchia, C.; Grassi, A.; Immirzi, A. *J. Am. Chem. Soc.* **1993**, *115*, 1160. (e) Calderazzo, F.; Ferri, I.; Pampaloni, G.; Troyanov, S. *J. Organomet. Chem.* **1996**, *518*, 189. (f) Gillis, D. J.; Quyoum, R.; Tudoret, M.-J.; Wang, Q.; Jeremic, D.; Roszak, A. W.; Baird, M. C. *Organometallics* **1996**, *15*, 3600. (g) Lancaster, S. J.; Robinson, O. B.; Bochmann, M.; Coles, S. J.; Hursthouse, M. B. *Organometallics* **1995**, *14*, 2456.

(26) The chelation of *o*-arylphenoxides to lanthanide metal centers has been observed in the solid state; see: (a) Deacon, G. B.; Feng, T.; Forsyth, C. M.; Gitlits, A.; Hockless, D. C. R.; Shen, O.; Skelton, B. W.; White, A. H. *J. Chem. Soc., Dalton Trans.* **2000**, 961 and references therein. (b) Deacon, G. B.; Fanwick, P. E.; Gitlits, A.; Rothwell, I. P.; Skelton, B. W.; White, A. H. *Eur. J. Inorg. Chem.* **2001**, *16*, 1505.

(27) (a) Hagadorn, J. R.; Arnold, J. *Angew. Chem., Int. Ed.* **1998**, *37*, 1729. (b) Cassani, M. C.; Duncalf, D. J.; Lappert, M. F. *J. Am. Chem. Soc.* **1998**, *120*, 12958.

(28) (a) Thewalt, U.; Stollmaier, F. *J. Organomet. Chem.* **1982**, *228*, 149. (b) Stollmaier, F.; Thewalt, U. *J. Organomet. Chem.* **1981**, *208*, 327. (c) Solari, E.; Floriani, C.; Chiesi-Villa, A.; Guastini, C. *J. Chem. Soc., Chem. Commun.* **1989**, 1747. (d) Solari, E.; Floriani, C.; Schenk, K.; Chiesi-Villa, A.; Rizzoli, C.; Rosi, M.; Sgamellotti, A. *Inorg. Chem.* **1994**, *33*, 2018. (e) Cotton, F. A.; Kibala, P. A.; Wojtczak, W. A. *J. Am. Chem. Soc.* **1991**, *113*, 1462. (f) Troyanov, S. I.; Rybakov, V. B. *Metalloorg. Khim.* **1992**, *5*, 1082. (g) Troyanov, S. I.; Meetsma, A.; Teuben, J. H. *Inorg. Chim. Acta* **1998**, *271*, 180. (h) Ozerov, O. V.; Patrick, B. O.; Ladipo, F. T. *J. Am. Chem. Soc.* **2000**, *122*, 6423. (i) Kupfer, V.; Thewalt, U. *Z. Anorg. Allg. Chem.* **2001**, *627*, 1423. (j) Gardner, T. G.; Girolami, G. S. *Angew. Chem., Int. Ed. Engl.* **1988**, *27*, 1693. (k) Troyanov, S. I.; Mach, K. *J. Organomet. Chem.* **1990**, *389*, 41. (l) Diamond, G. M.; Green, M. L. H.; Walker, N. W. *J. Organomet. Chem.* **1991**, *413*, C1. (m) Solari, E.; Musso, F.; Ferguson, R.; Floriani, C.; Chiesi-Villa, A.; Rizzoli, C. *Angew. Chem., Int. Ed. Engl.* **1995**, *34*, 1510. (n) Solari, E.; Musso, F.; Ferguson, R.; Floriani, C.; Chiesi-Villa, A.; Rizzoli, C. *Angew. Chem., Int. Ed. Engl.* **1995**, *34*, 1510. (o) Troyanov, S.; Pisarevsky, A.; Struchkov, Yu. T. *J. Organomet. Chem.* **1995**, *494*, C4.

(29) (a) Stollmaier, F.; Thewalt, U. *J. Organomet. Chem.* **1981**, *222*, 227. (b) Thewalt, U.; Stollmaier, F. *Angew. Chem., Int. Ed. Engl.* **1982**, *21*, 133. (c) Kesanli, B.; Fettinger, J.; Eichhorn, B. *Angew. Chem., Int. Ed.* **2001**, *40*, 2300. (d) Tayebani, M.; Feghali, K.; Gambarotta, S.; Yap, G. *Organometallics* **1998**, *17*, 4282. (e) Bandy, J. A.; Prout, K.; Cloke, F. G. N.; de Lemos, H. C.; Wallis, J. M. *J. Chem. Soc., Dalton Trans.* **1988**, 1475. (f) Goldberg, S. Z.; Spivack, B. D.; Stanley, G.; Eisenberg, R.; Braitsch, D. M.; Miller, J. S.; Abkowitz, M. *J. Am. Chem. Soc.* **1977**, *99*, 110. (g) Green, M. L. H.; O'Hare, D.; Watkin, J. G. *J. Chem. Soc., Chem. Commun.* **1989**, 698. (h) Calderazzo, F.; Pampaloni, G.; Rocchi, L.; Strahle, J.; Wurst, K. *J. Organomet. Chem.* **1991**, *413*, 91.

(30) (a) Bruck, M. A.; Copenhaver, A. S.; Wigley, D. E. *J. Am. Chem. Soc.* **1987**, *109*, 6525. (b) Arney, D. J.; Bruck, M. A.; Wigley, D. E. *Organometallics* **1991**, *10*, 3947. (c) Smith, D. P.; Stickler, J. R.; Gray, S. D.; Bruck, M. A.; Holmes, R. S.; Wigley, D. E. *Organometallics* **1992**, *11*, 1275. (d) Arney, D. J.; Wexler, P. A.; Wigley, D. E. *Organometallics* **1990**, *9*, 1282. (e) Arney, D. S. J.; Fox, P. A.; Bruck, M. A.; Wigley, D. E. *Organometallics* **1997**, *16*, 3421.

(31) Wexler, P. A.; Wigley, D. E.; Koerner, J. B.; Albright, T. A. *Organometallics* **1991**, *10*, 2319.

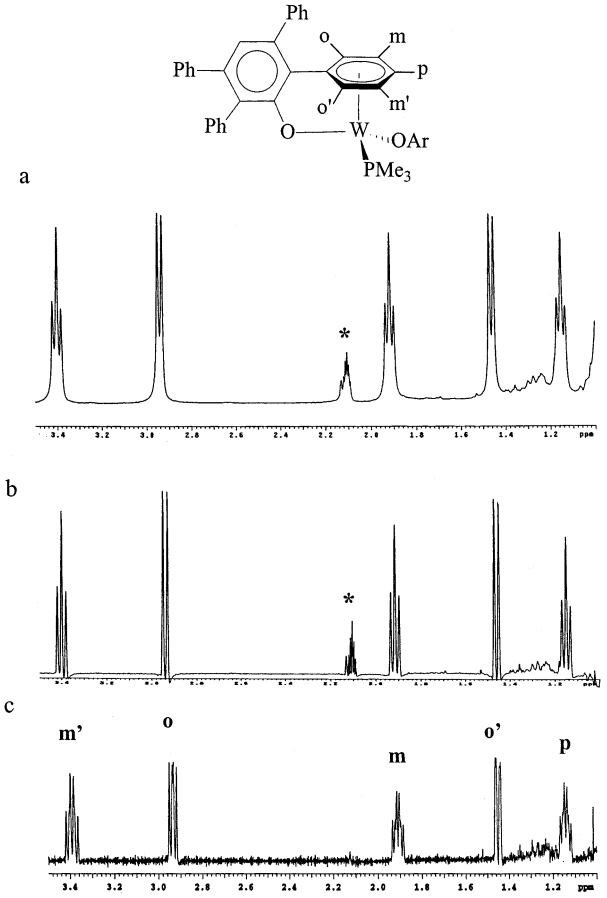

Figure 3. ^{1}H NMR spectra (toluene-d_8, −30 °C) of the η^6-C_6H_5 protons in [W(OC_6HPh_3-η^6-C_6H_5)(OC_6HPh_4-2,3,5,6)(PMe_3)] (**4b**): (a) δ 1.0−3.5 ppm region, ^{31}P decoupled; (b) ^{31}P decoupled spectrum with use of weighing functions; (c) ^{31}P coupled with solvent suppression and weighing functions. The asterisk indicates protio impurities within the solvent.

pairs of protons. The upfield shifting of these arene protons is a consequence of the π-coordination to the metal center. This upfield shifting is also enhanced by the presence of the adjacent 2,3,5,6-tetraphenylphenoxide ligand. Previous work has demonstrated that the ortho phenyl rings of such ligands cause a diamagnetic shielding of the protons of adjacent ligands.[8a]

We have undertaken a number of NMR experiments in order to gain as much information as possible about the π-bound arene resonances of the PMe_3 derivative **4b**. The use of homodecoupling and 2D COSY experiments has allowed the ortho, meta, and para protons to be assigned. However, these experiments on their own do not allow unequivocal assignment of the nonequivalent pairs of ortho and meta protons on the ring: i.e., which pair is on the side of the ring adjacent to the terminal aryloxide and which pair is adjacent to the phosphine ligand. From the ^{1}H{^{31}P} NMR spectrum at −30 °C (Figure 3) the $^3J_{H-H}$ coupling constants could be derived by simulation of the observed spectrum. Simulation of the ^{31}P-coupled spectrum then allowed measurement of the $^3J_{P-H}$ coupling constants. Finally, low-temperature NOE difference experiments involving irradiation of the PMe_3 protons allowed the unequivocal assignment of the five aromatic protons attached to the η^6-bound phenyl ring (Table 2).

Table 2. Measured Coupling Constants for 4b[a]

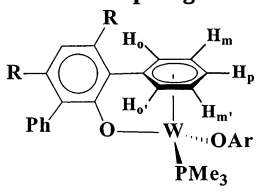

proton	shift (ppm)	$^3J(^1H-^1H)$[b]	$^3J(^1H-^1H)$[c]	$^3J(^{31}P-^1H)$[c]
$H_{m'}$	3.37	5.57	5.53	4.18
H_o	2.92	5.95	5.84	4.04
H_m	1.89	5.88	5.86	3.31
$H_{o'}$	1.45	5.95	5.88	1.62
H_p	1.02	5.57	5.56	3.37

[a] Errors in measured coupling constants on the Varian Unity Inova 300 are ±0.15 Hz. [b] Average measured coupling (in Hz) from the ^{1}H{^{31}P} NMR experiment at −30 °C. [c] Average measured coupling (in Hz) from the ^{1}H NMR experiment at −30 °C using weighing functions.

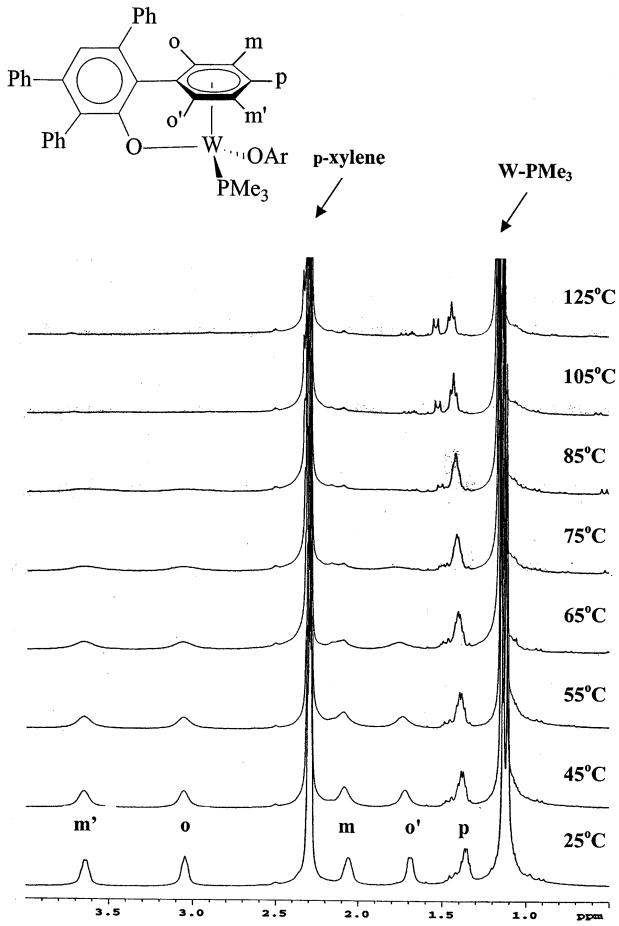

Figure 4. High-temperature ^{1}H NMR spectra (*p*-xylene-d_{10}, δ 0.0−4.0 ppm) of the η^6-C_6H_5 protons in [W(OC_6HPh_3-η^6-C_6H_5)(OC_6HPh_4-2,3,5,6)(PMe_3)] (**4b**).

The temperature dependence of the ^{1}H NMR spectra is highly informative. As the temperature of a solution of **4b** in perdeutero-*p*-xylene is raised, the ortho and meta proton resonances broaden. At 125 °C they have collapsed completely into the baseline. Unfortunately, high-temperature limiting spectra could not be obtained due to thermal decomposition to a compound discussed below. However, it can be seen (Figure 4) that although exchange of pairs of ortho and meta protons is occurring on the NMR time scale, the para proton resonance remains sharp. We interpret the changes in the NMR

Scheme 2

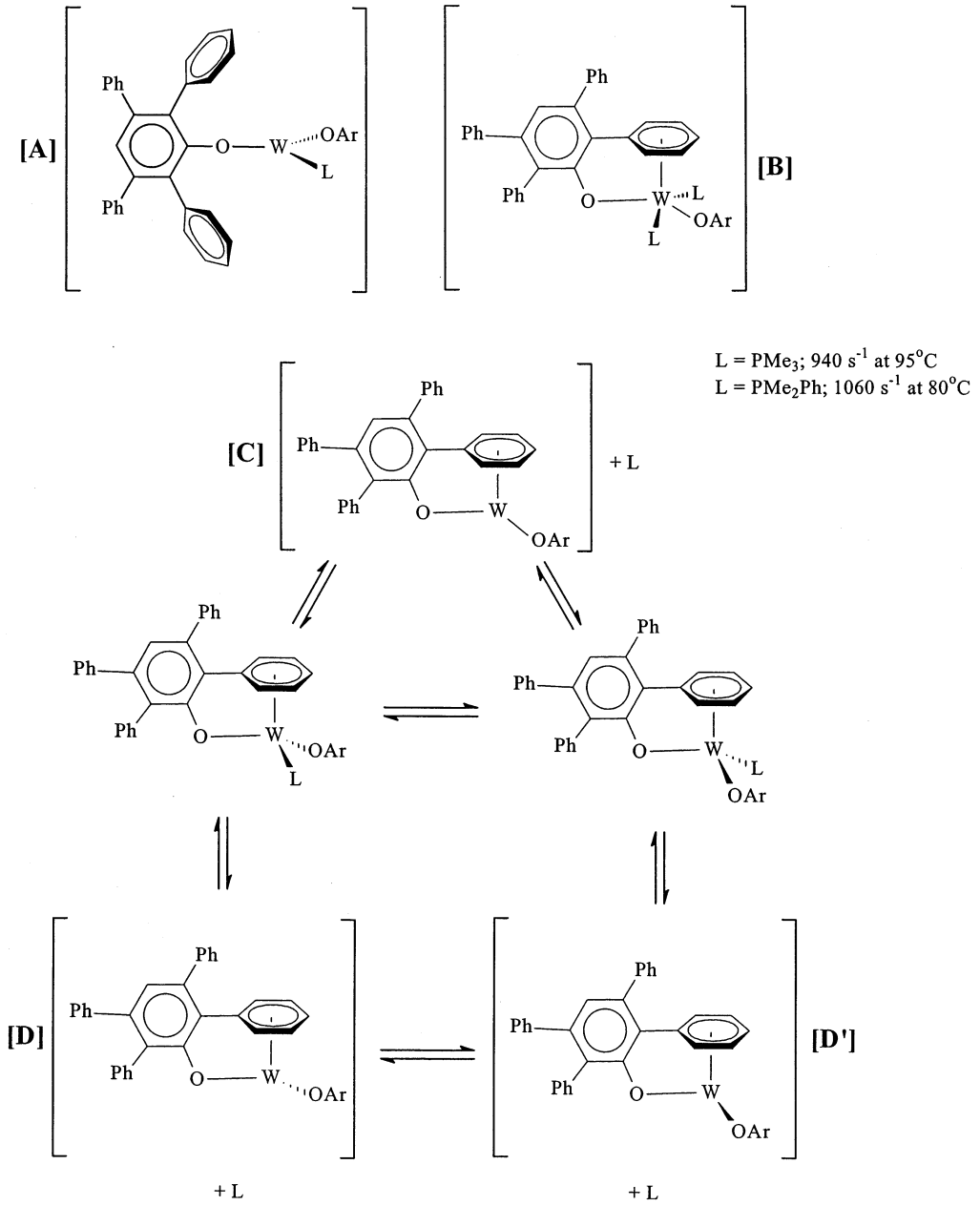

spectrum as reflecting a fluxional process for the molecule in which the sides of the bound arene ring are becoming equivalent (Scheme 2). Furthermore, the sharp resonance for the para proton implies that dissociation of the bound arene ring does not take place. If arene ring dissociation followed by rotation was the mechanism of o,o′ and m,m′ exchange (intermediate [A] in Scheme 2), then one would expect the bound arene to exchange with the other ortho phenyl rings. It therefore appears that exchange of the phosphine and terminal aryloxide ligands is taking place. This could occur via two distinct pathways. If one ignores oxygen-p to metal-d π-bonding, then **4**−**6** are formally 16-electron compounds. The previously isolated compounds [W(OC_6-HPh_3-η^6-C_6H_5)(X)($L)_2$] (X = H, Cl; L = tertiary phosphine) contain a hydrido or chloro ligand in place of an aryloxide and form 18-electron bis(phosphine) adducts.[32]

It therefore is feasible that the exchange process occurs through an associative pathway via the 18-electron intermediate [B] in Scheme 2. This would require the exchange to be catalyzed by trace amounts of free phosphine in solution. However, we find that adding excess PMe_3 to solutions of **4b** does not lead to an increase in exchange of nonequivalent ortho and meta protons; i.e., no increase in line broadening is observed in the ^{1}H NMR spectra. However, we do know that exchange of free and coordinated phosphine can occur rapidly. Hence, addition of PMe_2Ph to a solution of **4b** rapidly sets up equilibrium between **4b**/**4e** and PMe_3/PMe_2Ph. Hence, we propose that the fluxional process occurs via a dissociative exchange of phosphine ligand. Furthermore, exchange of the nonequivalent ortho and para protons is not inhibited by added phosphine, indicating that the two-legged piano-stool intermediate must contain a mirror plane ([C] in Scheme 2). A preequilibrium step to generate a species of lower

(32) Kerschner, J. L.; Torres, E. M.; Fanwick, P. E.; Rothwell, I. P.; Huffman, J. C. *Organometallics* **1989**, *8*, 1424.

Scheme 3

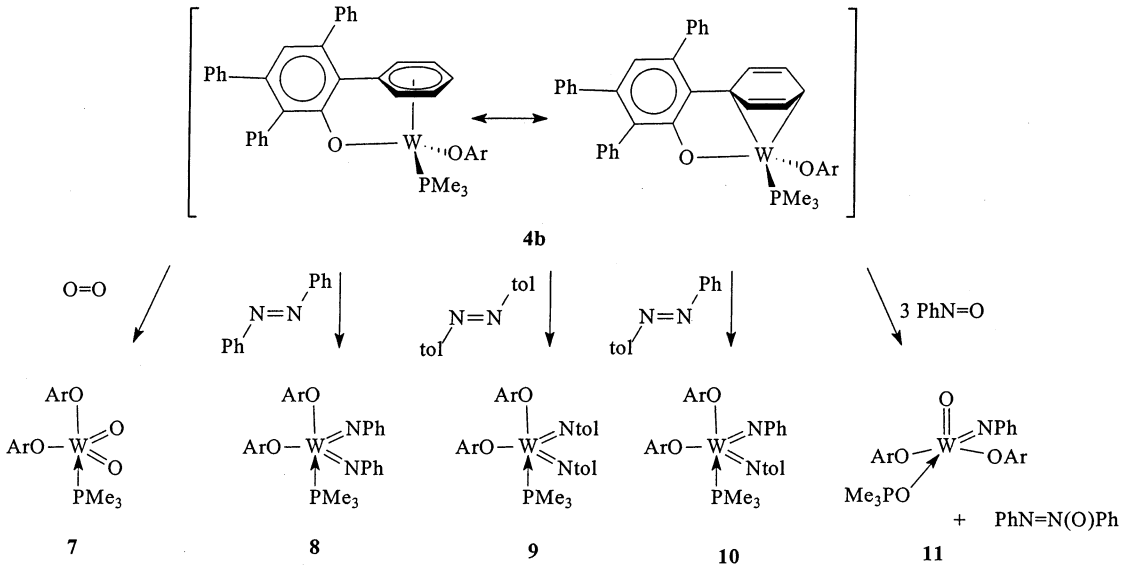

symmetry followed by an "inversion" process ([D, D′], Scheme 2) would lead to inhibition by added phosphine. The geometry proposed for the intermediate is strikingly similar to that found for the bis(aryloxide) [Ta(η^6-C_6Et_6)($OC_6H_3Pr^i_2$-2,6)$_2$] reported by Wigley,[31] although the tungsten compound has one extra electron. Although it is unsatisfying that high-temperature limiting spectra could not be obtained, the o,o′ and m,m′ exchange rate can be estimated at the coalescence temperatures. For the PMe_3 derivative **4b** this is estimated as 940 s^{-1} at 95 °C. The coalescence temperature for the PMe_2Ph derivative is slightly lower, yielding an exchange rate of 1060 s^{-1} at 80 °C. This trend is consistent with a phosphine dissociative exchange pathway.

Synthesis and Solid-State Structure of Oxo and Arylimido Products. In this section we describe the utility of **4b** for the synthesis of corresponding oxo and arylimido compounds. Preliminary studies on the reaction of **4a** with O_2 and aryldiazines showed the formation of the corresponding bis(oxo) and bis(imido) derivatives.[11a] Spectroscopic data showed the lack of coordination of the dppm ligand to the W(VI) products. A crystal structure of the compound [W(OC_6HPh_4-2,3,5,6)$_2$(=NPh)$_2$] showed a pseudo-tetrahedral W(VI) metal center with terminal aryloxides and no coordinated phosphine ligand. However, the dppm derivative proved unsuitable for mechanistic/kinetic studies due to a number of factors, including the low solubility of both **4a** and the free dppm produced during the reaction. Furthermore, imido compounds produced via cleavage of diazines were found to undergo ligand exchange reactions.[11a] Related ligand exchange reactions have been observed for tetrahedral molybdenum compounds and studied in detail.[33] These problems were resolved by utilizing the more soluble PMe_3 compound **4b**, which will react with dioxygen, aryldiazines, and nitrosobenzene to form a series of oxo and imido derivatives of W(VI) that are five-coordinate, containing coordinated PMe_3, and do not undergo facile intermolecular scrambling of ligands (Scheme 3).

(33) Blackmore, I. J.; Gibson, V. C.; Graham, A. J.; Jolly, M.; Marshall, E. L.; Ward, B. P. *Dalton* **2001**, 3242.

A deep green C_6D_6 solution of **4b** rapidly became brown upon exposure to an atmosphere of O_2 at ambient temperatures. Analysis by ^1H and ^{31}P NMR showed aromatic resonances for terminal aryloxide ligands and a coordinated PMe_3 ligand. Structural analysis of crystals obtained from benzene/hexane confirms the formulation as the W(VI) dioxo species **7** (Scheme 3) with a pentagonal-bipyramidal geometry about tungsten. The coordinated PMe_3 ligand occupies an axial site, trans to one of the aryloxo ligands (Figure 5, Table 3). Reaction of **4b** with the *trans*-diazines PhN═NPh, TolN═NTol, and PhN═NTol (Tol = 4-methylphenyl) led to the corresponding bis(arylimido) derivatives **8**−**10** (Scheme 3). The reactions were noticeably slower than the dioxygen reaction and were amenable to kinetic studies (see below). Besides evidence for the coordinated PMe_3 ligand, the ^1H NMR spectra of **8**−**10** showed

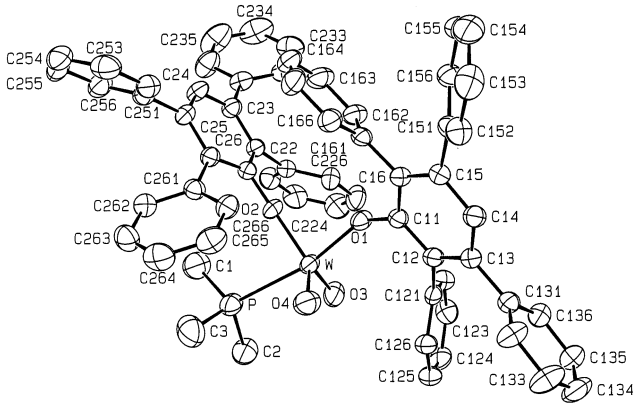

Figure 5. Molecular structure of [W(OC_6HPh_4-2,3,5,6)$_2$-(O)$_2$(PMe_3)] (**7**).

Table 3. Selected Bond Distances (Å) and Angles (deg) for [W(O)$_2$(OC_6HPh_4-2,3,5,6)$_2$(PMe_3)] (7)

W-O(1)	1.943(3)	W−O(4)	1.709(4)
W−O(2)	1.902(3)	W−P	2.638(1)
W−O(3)	1.710(3)		
O(2)−W−O(1)	87.5(1)	O(1)−W−P	167.42(9)
O(3)−W−O(2)	119.6(2)	O(4)−W−P	87.12(13)
O(4)−W−O(2)	128.1(2)	W−O(1)−C(11)	137.0(3)
O(3)−W−O(4)	108.5(2)	W−O(2)−C(21)	176.6(3)

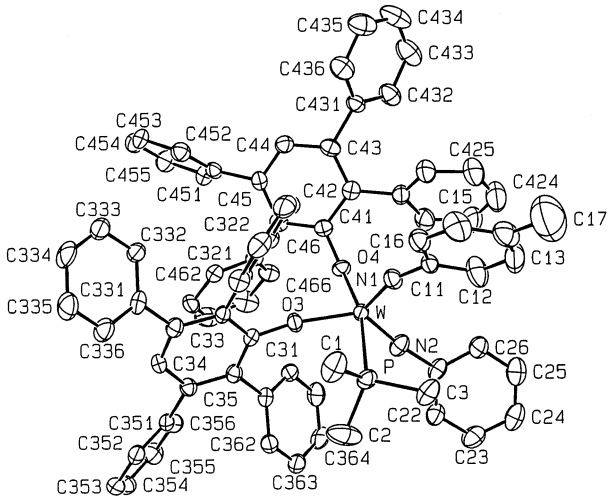

Figure 6. Molecular structure of $[W(OC_6HPh_4\text{-}2,3,5,6)_2(NPh)(Ntol)(PMe_3)]$ (**10**).

Table 4. Selected Bond Distances (Å) and Angles (deg) for $[W(NPh)(Ntol)(OC_6HPh_4\text{-}2,3,5,6)_2(PMe_3)]$ (10)

W−N(1)	1.751(5)	W−O(4)	2.010(3)
W−N(2)	1.774(5)	W−P	2.538(1)
W−O(3)	1.965(4)		
N(1)−W−N(2)	109.4(2)	N(1)−W−P	84.5(2)
N(1)−W−O(3)	117.6(2)	O(4)−W−P	166.2 (1)
N(2)−W−O(3)	129.2(2)	W−O(3)−C(31)	170.5(3)
N(2)−W−O(4)	99.3(2)	W−O(4)−C(41)	134.0(3)

distinctive aromatic resonances slightly upfield of the aryloxide proton resonances. These can be assigned to the aromatic protons of the arylimido groups, shifted upfield by the diamagnetic anisotropy of the adjacent 2,3,5,6-tetraphenylphenoxide ligands. The ^{1}H NMR spectrum of **10** showed no evidence for the formation of either **8** or **9** in the reaction mixture. The mixed-imido species **10** was also crystallized and shown to contain a structure similar to that of **7** with the phenyl- and tolylimido ligands both equatorial (Figure 6, Table 4).

The reaction of **4b** with nitrosobenzene was found to generate a significantly different compound. In this case the ^{31}P NMR spectrum of the product showed a broad resonance at δ +32.7 ppm, considerably downfield of the region found for the PMe_3 ligands in **7**−**10**. This new product **11** (Scheme 3) was structurally characterized and shown to contain an $OPMe_3$ ligand bound to tungsten (Figure 7, Table 5). Analysis of the reaction mixture showed proton resonances in the aromatic region identical with those for an authentic sample of oxazoline. In an independent NMR experiment it was shown that nitrosobenzene reacts with PMe_3 to produce the phosphine oxide and oxazoline. The molecular structure of **11** contains a geometry about tungsten best described as square pyramidal. An oxo group occupies the axial site, with the phosphine oxide adduct located trans to a basal phenylimido ligand.

Compound **4b** was also found to ring open the substrates pyridazine, benzo[*c*]cinnoline, and phthalazine to form **12**−**14**, respectively (Scheme 4). These constrained *cis*-diazo substrates were found to react significantly faster with **4b** than the trans diazines used in Scheme 3. However, evidence was obtained by ^{1}H and ^{31}P NMR for the formation of a deep blue-green intermediate species which was stable for hours at −30 °C.

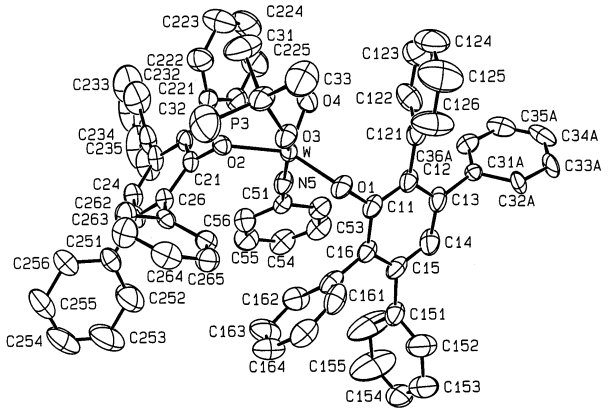

Figure 7. Molecular structure of $[W(OC_6HPh_4\text{-}2,3,5,6)_2(NPh)(O)(OPMe_3)]$ (**11**).

Table 5. Selected Bond Distances (Å) and Angles (deg) for $[W(O)(NPh)(OC_6HPh_4\text{-}2,3,5,6)_2(OPMe_3)]$ (11)

W−O(1)	1.966(4)	W−O(4)	1.694(4)
W−O(2)	1.973(4)	W−N(5)	1.752(5)
W−O(3)	2.117(4)		
O(1)−W−O(2)	139.9(2)	O(1)−W−N(5)	94.4(2)
O(1)−W−O(3)	77.9(2)	O(4)−W−N(5)	104.1(2)
O(1)−W−O(4)	109.1(2)	O(2)−W−N(5)	95.4(2)
O(3)−W−O(2)	78.6(2)	O(3)−W-N(5)	158.0(2)
O(2)−W−O(4)	106.0(2)	W−O(1)−C(11)	124.6(4)
O(4)−W−−(3)	97.9(2)	W−O(2)−C(21)	125.1(3)

Unfortunately this intermediate could not be characterized fully, and it converted rapidly to **13** at higher temperatures. The product diaza metallacyclic products **12**−**14** are spectroscopically similar to **8**−**10**. Crystallographic studies of **12**−**14** (Figures 8−10, Tables 6−8) showed a tbp geometry in all cases similar to that found in **10**.[34] In compound **13** the two benzene rings fused to the diaza metallacycle are twisted with a torsion angle of 33°. This generates a puckering of the seven-membered ring. In contrast, the products of ring opening of pyridazine, **12**, and phthalazine, **14**, have planar seven-membered rings.

The structural parameters for the five-coordinate oxo and imido compounds **7** and **10**−**14** are of considerable interest. The W−OAr distances span the narrow range of 1.902(3)−2.010(3) Å. This range is comparable to that for other W(VI) aryloxides in the literature.[1] There are a large number of terminal oxo and imido derivatives of W(VI) now known. However, analysis of the Cambridge Structural Database shows that few five-coordinate adducts of this type have been structurally characterized, although there is a much larger set of such molybdenum compounds. In the phosphine adducts **7** and **10** the O═W═O and N═W═N angles are 108 and 109°, respectively. This compares well with N═W═N angles found in the related molecules $[W(=NBu^t)_2\{OC(CF_3)_2\ C(CF_3)_2O\}(H_2NBu^t)]$ (110°),[35] $[W\{=NSi(Bu^t)_3\}_2Cl_2(py)]$ (111°),[36] and $[W(=NSiMe_3)_2Cl_2(PMePh_2)]$ (110°).[37]

(34) A nine-membered ring containing a tungsten bis(imido) function has been reported, $[Cp^*WCl(NC_6H_4{-}CH_2CH_2{-}C_6H_4N)]$; see: Redshaw, C.; Gibson, V. C.; Clegg, W.; Edwards, A. J.; Miles, B. *J. Chem. Soc., Dalton Trans.* **1997**, 3343.

(35) Chan, D. M.-T.; Fultz, W. C.; Nugent, W. A.; Roe, D. C.; Tulip, T. H. *J. Am. Chem. Soc.* **1985**, *107*, 251.

(36) Holmes, S. M.; Schafer, D. F., II; Wolczanski, P. T.; Lobkovsky, E. B. *J. Am. Chem. Soc.* **2001**, *123*, 10571.

(37) Lichtenhan, J. D.; Critchlow, S. C.; Doherty, N. M. *Inorg. Chem.* **1990**, *29*, 439.

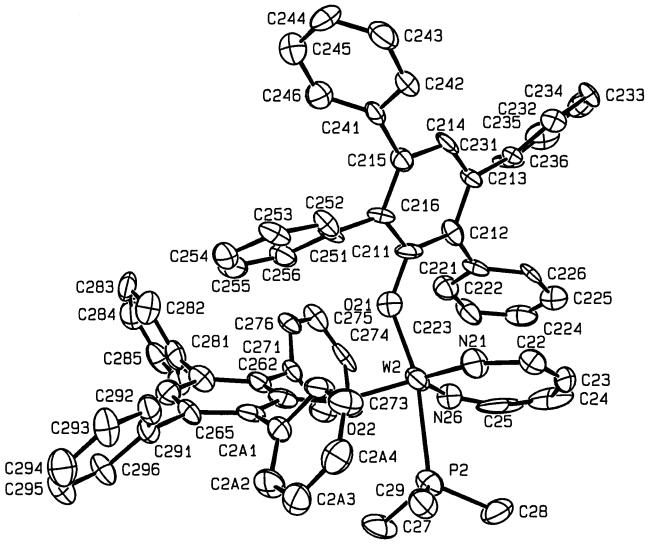

Figure 8. Molecular structure of $[W(OC_6HPh_4\text{-}2,3,5,6)_2\{NCHCHCHCHN\}(PMe_3)]$ (**12**).

Table 6. Selected Bond Distances (Å) and Angles (deg) for $[W(OC_6HPh_4\text{-}2,3,5,6)_2\{NCHCHCHCHN\}(PMe_3)]$ (12)

molecule 1		molecule 2	
W(1)−N(11)	1.740(7)	W(2)−N(21)	1.783(7)
W(1)−N(16)	1.744(7)	W(2)−N(26)	1.701(7)
W(1)−O(11)	1.961(6)	W(2)−O(21)	1.965(5)
W(1)−O(12)	1.970(6)	W(2)−O(22)	1.969(6)
W(1)−P(1)	2.580(2)	W(2)−P(2)	2.558(2)
N(11)−C(12)	1.39(1)	N(21)−C(22)	1.37(1)
N(16)−C(15)	1.42(1)	N(26)−C(25)	1.34(2)
C(12)−C(13)	1.38(1)	C(22)−C(23)	1.38(1)
C(13)−C(14)	1.43(1)	C(23)−C(24)	1.46(1)
C(14)−C(15)	1.34(1)	C(24)−C(25)	1.39(2)
O(11)−W(1)−O(12)	88.8(2)	O(21)−W(2)−O(22)	86.6(2)
N(11)−W(1)−N(16)	101.0(4)	N(21)−W(2)−N(26)	103.6(4)
N(11)−W(1)−O(11)	102.3(3)	N(21)−W(2)−O(21)	101.0(3)
N(11)−W(1)−O(12)	127.0(3)	N(21)−W(2)−O(22)	135.7(3)
N(16)−W(1)−O(11)	104.3(3)	N(26)−W(2)−O(21)	103.1(3)
N(16)−W(1)−O(12)	126.5(3)	N(26)−W(2)−O(22)	117.2(3)
N(11)−W(1)−P(1)	84.9(2)	N(21)−W(2)−P(2)	86.8(2)
N(16)−W(1)−P(1)	83.5(2)	N(26)−W(2)−P(2)	86.5(2)
P(1)−W(1)−O(11)	168.0(2)	P(2)−W(2)−O(21)	165.7(2)
P(1)−W(1)−O(12)	79.2(2)	P(2)−W(2)−O(22)	79.5(2)
W(1)−O(11)−C(111)	140.5(5)	W(2)−O(21)−C(211)	135.1(5)
W(1)−O(12)−C(161)	162.4(5)	W(2)−O(22)−C(261)	159.9(5)
W(1)−N(11)−C(12)	143.0(7)	W(2)−N(21)−C(22)	144.2(7)
W(1)−N(16)−C(15)	141.2(7)	W(2)−N(26)−C(25)	135.4(8)
N(11)−C(12)−C(13)	122.5(10)	N(21)−C(22)−C(23)	121.2(10)
C(12)−C(13)−C(14)	135.1(11)	C(22)−C(23)−C(24)	133.5(10)
C(13)−C(14)−C(15)	131.7(11)	C(23)−C(24)−C(25)	129.0(11)
N(16)−C(15)−C(14)	125.4(10)	N(26)−C(25)−C(24)	132.5(13)

These all contain the oxo or imido groups equatorial in a tbp structure. A slightly smaller angle of 104° is found for square-pyramidal **11**. The W═O and W═N distances within **7**, **10**, and **11** appear to be in the range reported for other W(VI) derivatives of these ligands. The structural parameters for the three diazametallacyclic compounds **12**−**14** are highlighted in Scheme 5. The presence of the seven-membered ring constrains the N═W═N angles to slightly smaller values of 101, 98, and 99°, respectively, compared to the terminal bis(imido) species **10**. There are two possible resonance forms which can be drawn for **12**−**14** (Scheme 5). In form **A** there is a d^0-W(VI) metal center with a 2,7-diazatungstahepta-1,3,5,7-tetraene ring and two tungsten−imido bonds. In contrast, form **B** has a formally d^2-W(IV) metal center

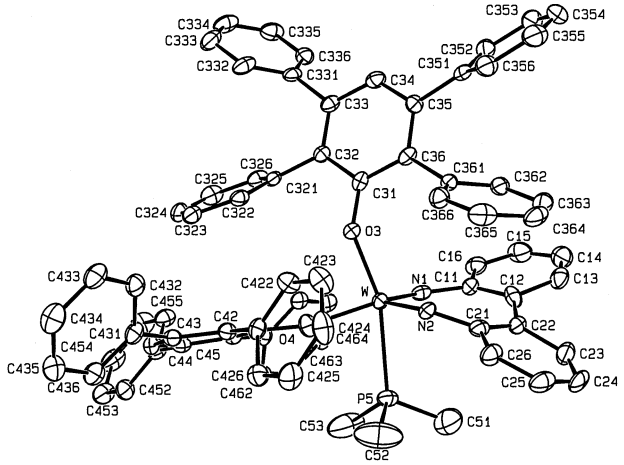

Figure 9. Molecular structure of $[W(OC_6HPh_4\text{-}2,3,5,6)_2(NC_{12}H_8N)(PMe_3)]$ (**13**).

Table 7. Selected Bond Distances (Å) and Angles (deg) for $[W(OC_6HPh_4\text{-}2,3,5,6)_2(NC_{12}H_8N)(PMe_3)]$ (13)

W−N(1)	1.753(4)	N(1)−C(11)	1.393(6)
W−N(2)	1.751(4)	N(2)−C(21)	1.390(6)
W−O(3)	1.991(3)	C(11)−C(12)	1.426(7)
W−O(4)	1.987(3)	C(12)−C(22)	1.496(7)
W−P(5)	2.566(1)	C(21)−C(22)	1.426(6)
O(3)−W−O(4)	85.8(1)	N(2)−W−P(5)	84.6(1)
N(1)−W−N(2)	97.9(2)	P(5)−W−O(3)	162.52(9)
N(1)−W−O(3)	103.7(1)	P(5)−W−O(4)	76.71(9)
N(1)−W−O(4)	134.5(2)	W−O(3)−C(31)	144.6(3)
N(2)−W−O(3)	105.2(1)	W−O(4)−C(41)	166.4(3)
N(2)−W−O(4)	122.8(2)	W−N(1)−C(11)	143.8(3)
N(1)−W−P(5)	88.9(1)	W−N(2)−C(21)	143.0(3)
C(13)−C(12)-C(22)−C(23)[a]			−31.2(6)

[a] Torsion angle.

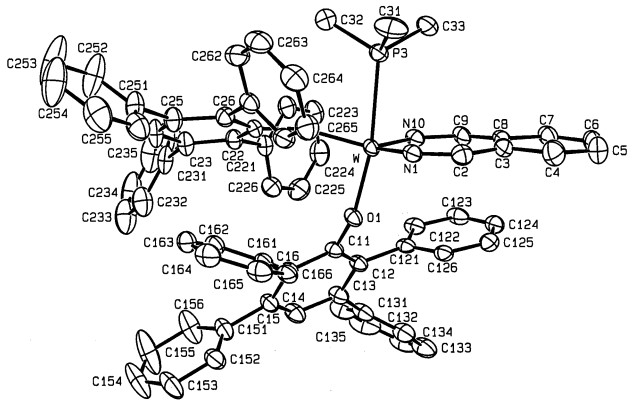

Figure 10. Molecular structure of $[W(OC_6HPh_4\text{-}2,3,5,6)_2\{NCH(C_6H_4)CHN\}(PMe_3)]$ (**14**).

with a 2,7-diazatungstahepta-2,4,6-triene ring. The structural parameters for **12** and **13** (Scheme 5) are consistent with the bis(imido) form. There is a definite lengthening of the W−N distances in **14**, with distances around the ring showing a perturbation toward resonance form **B**. The W−N distances are not, however, as long as those found for single bonds such as in known [W−N═C]-containing structures. For example, the W−N distances of 1.791(3) and 1.797(3) Å in **14** are shorter than those in $[CpMo(CO)_2(N{=}CBu^t_2)]$ (1.892 Å)[38] and [(tpb)W(CO)(η^2-PhCCMe)(N═CMePh)] (1.898 Å),[39] which contain single M−N═C bonds.

Scheme 4

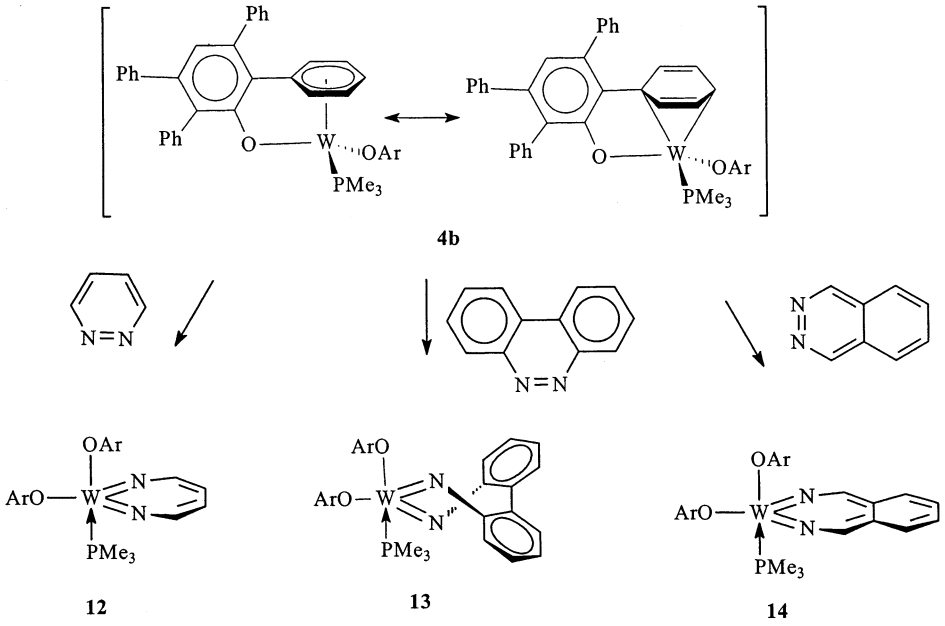

Table 8. Selected Bond Distances (Å) and Angles (deg) for [W(OC$_6$HPh$_4$-2,3,5,6)$_2${NCH(C$_6$H$_4$)CHN}(PMe$_3$)] (14)

W−N(1)	1.797(3)	C(2)−C(3)	1.417(5)
W−N(10)	1.791(3)	C(3)−C(4)	1.434(5)
W−O(1)	1.982(2)	C(3)−C(8)	1.456(5)
W−O(2)	1.959(2)	C(4)−C(5)	1.363(6)
W−P(3)	2.565(1)	C(5)−C(6)	1.400(6)
N(1)−C(2)	1.326(5)	C(6)−C(7)	1.347(6)
N(10)−C(9)	1.335(4)	C(7)−C(8)	1.449(5)
		C(8)−C(9)	1.411(5)
O(2)−W−O(1)	91.3(1)	P(3)−W−O(2)	80.07(8)
N(1)−W−N(10)	98.7(1)	W−O(1)−C(11)	143.0(2)
N(1)−W−O(2)	135.0(1)	W−O(2)−C(21)	162.0(2)
N(10)−W−O(1)	107.0(1)	W−N(1)−C(2)	142.9(2)
N(1)−W−O(1)	95.1(1)	W−N(10)−C(9)	141.4(3)
N(10)−W−O(2)	121.8(1)	N(1)−C(2)−C(3)	128.6(3)
N(10)−W−P(3)	83.6(9)	C(2)−C(3)−C(8)	128.8(3)
N(1)−W−P(3)	86.34(9)	C(3)−C(8)−C(9)	130.1(3)
P(3)−W−O(1)	168.90(7)	C(8)−C(9)−N(10)	129.3(3)

Kinetic and Mechanistic Studies. The reactions of **4b** with the various substrates represents the overall four-electron reduction of O═O, N═N, and N═O bonds by the d^4-W(II) metal center. A reaction of this type could be imagined to take place via numerous possible pathways. A theoretical analysis of the reaction of the model compound [(η^6-C$_6$H$_6$)W(OH)$_2$(PH$_3$)] with *cis*-HN═NH shows there to be no electronic barriers to the reaction occurring in a purely intramolecular fashion at one metal center.[11] There is precedence for the single-site cleavage of diazo substrates into bis(imido) products in the work of Burns et al.[40] There is strong precedence for the cleavage of azobenzene by d^2-metal fragments to occur via bimolecular intermediates.[41−43] Furthermore, the fundamentally important activation and cleavage of dioxygen typically occurs at more than one metal center.[44] Analysis of the product stoichiometry implies that the reactions involving **4b** are occurring at a single metal center. A number of earlier studies

Scheme 5

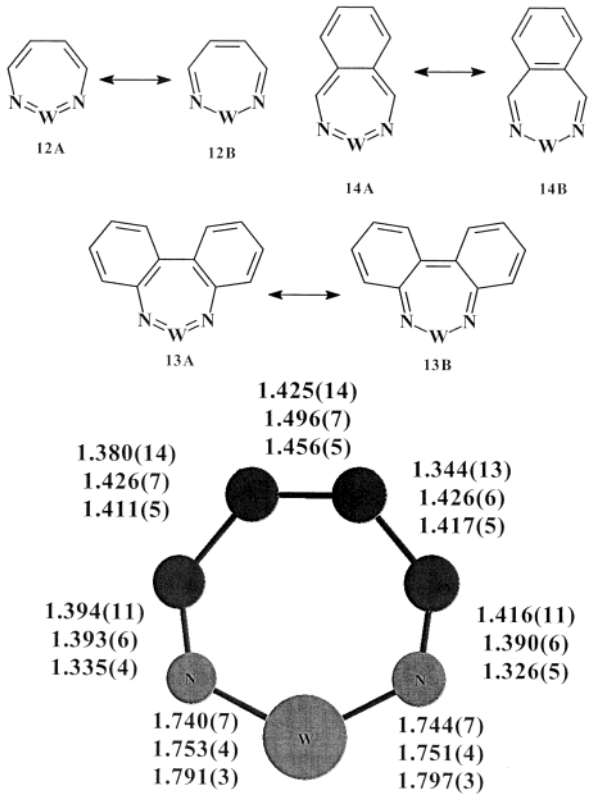

(38) Shearer, H. M. M.; Sowerby, J. D. *J. Chem. Soc., Dalton Trans.* **1973**, 2629.

(39) Francisco, L. W.; White, P. S.; Templeton, J. L. *Organometallics* **1996**, *15*, 5127.

(40) (a) Peters, R. G.; Warner, B. P.; Burns, C. J. *J. Am. Chem. Soc.* **1999**, *121*, 5585. (b) Warner, B. P.; Scott, B. L.; Burns, C. J. *Angew. Chem., Int. Ed.* **1998**, *37*, 959. (c) Arney, D. S. J.; Burns, C. J. *J. Am. Chem. Soc.* **1995**, *117*, 9448.

(41) (a) Cotton, F. A.; Duraj, S. A.; Roth, W. J. *J. Am. Chem. Soc.* **1984**, *106*, 4749. (b) Hill, J. E.; Profilet, R. D.; Fanwick, P. E.; Rothwell, I. P. *Angew. Chem., Int. Ed. Engl.* **1990**, *29*, 664. (c) Hill, J. E.; Fanwick, P. E.; Rothwell, I. P. *Inorg. Chem.* **1991**, *30*, 1143. (d) Durfee, L. D.; Hill, J. E.; Fanwick, P. E.; Rothwell, I. P. *Organometallics* **1990**, *9*, 75. (e) Zambrano, C. H.; Fanwick, P. E.; Rothwell, I. P. *Organometallics* **1994**, *13*, 1174.

(42) (a) Walsh, P. J.; Hollander, F. J.; Bergman, R. G. *J. Am. Chem. Soc.* **1990**, *112*, 894. (b) Walsh, P. J.; Hollander, F. J.; Bergman, R. G. *J. Organomet. Chem.* **1992**, *428*, 13. (c) Aubart, M. A.; Bergman, R. G. *Organometallics* **1999**, *18*, 811.

Scheme 6

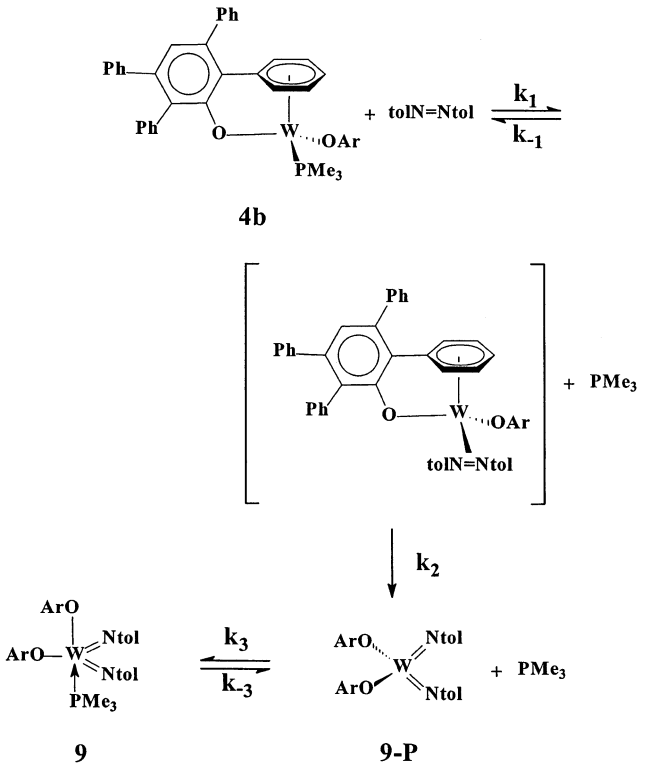

If k_1/k_{-1} small and k_1, k_{-1},k_3, k_{-3}>> k_2 then

$$\frac{-d[4b]}{dt} = k_2\left(\frac{k_1}{k_{-1}}\right)\frac{[4b]\,[tolN{=}Ntol]}{[PMe_3]}$$

and

$$[PMe_3] = \left(\frac{k_{-3}}{k_3}\right)\frac{[9]}{[9\text{-}P]}$$

indicated a significant barrier to the conversion of d^2-peroxo species into the corresponding d^0-bis(oxo) compound. In one case it was found that the symmetry of the system precluded the flow of the two metal-based electrons into the O−O σ^* orbital.[45] Another significant discovery by Maatta and Wentworth was the complete lack of thermal or photochemical interconversion of the η^2-nitrosobenzene complex $[Mo(ONPh)(S_2CNEt_2)_2]$ and the oxo imido valence isomer $[Mo(O)(NPh)(S_2CNEt_2)_2]$.[46]

To gain even more insight into this reactivity, we have carried out a kinetic study of the reaction of **4b** with *trans*-4,4′-dimethylazobenzene. The reaction was monitored via ^{1}H NMR spectroscopy. During the course of the reaction, only the reagents and product were observed. No intermediate species were detectable by NMR. The reaction was also strongly inhibited by the addition of free PMe_3. A series of kinetic runs were carried out by monitoring the disappearance of the proton signals for **4b** as a function of time while varying the concentration of both **4b** and *trans*-4,4′-dimethylazobenzene. The resulting curves were successfully fit to a kinetic model using a simulation program.[47] The model used is shown in Scheme 6. We propose an initial fast preequilibrium involving exchange of coordinated PMe_3 for the diazine. This equilibrium lies to the left and accounts for the inhibition by added phosphine. Whether this ligand exchange occurs via an associative or a dissociative pathway is unknown. However, we do know that phosphine exchange as monitored by the fluxionality of **4b** is dissociative. The diazine intermediate then undergoes a relatively slow conversion to the bis(imido) complex. To fit the kinetic data accurately, it was found necessary to include the final equilibrium between the bis(imido) complex and PMe_3 to form **9**. We know that this last step is fast compared to the overall rate of the reaction. The ^{1}H NMR spectrum of the product **9** shows a single broad resonance for the PMe_3 group at ambient temperatures. When the temperature is lowered, the resonance shifts further upfield and sharpens. The broadening and downfield shift upon raising the temperature is due to the fast (on the NMR time scale) exchange of free and coordinated PMe_3 as well as a shift in the equilibrium toward free PMe_3 (which resonates downfield of the coordinated ligand). If the model is correct, then fitting of individual kinetic runs should yield a consistent set of values for the terms $\{k_2k_1/k_{-1}\}$ and the final equilibrium constant $\{k_3/k_{-3}\}$. The results (Figure 11) for data obtained at 28.0(5) °C support the kinetic model. An independent estimate of $\{k_3/k_{-3}\}$ was obtained using the PMe_3 chemical shift observed in the ^{1}H NMR spectrum of **9** at 28 °C and

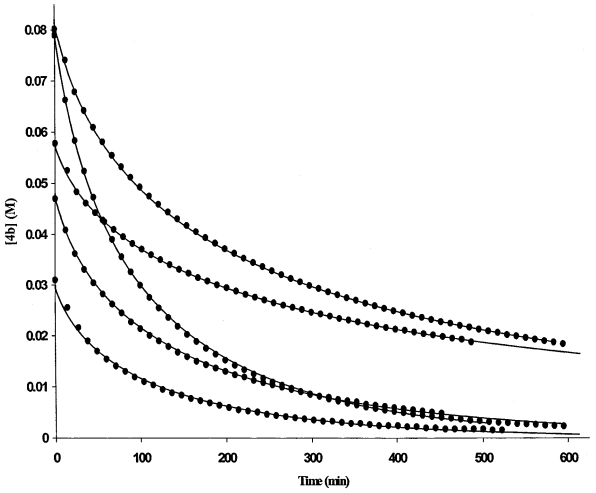

Exp.	$[W]_0$/M	$[A]_0$/M	$k_2(k_1/k_{-1})$ (10^6)	k_3/k_{-3} (10^{-3})
1	0.082	0.100	1.69	8.70
2	0.080	0.230	1.70	8.33
3	0.058	0.064	1.70	8.33
4	0.048	0.126	1.73	8.51
5	0.030	0.118	1.68	8.00
Ave.			1.70(2)	8.4(3)

Figure 11. Plots of [**4b**] vs time for various initial concentrations of **4b**, $[W]_0$ and Tol−N=N−Tol, $[A]_0$ as monitored by ^{1}H NMR in C_6D_6 at 28.0(5) °C. The data is fit to the kinetic model in Scheme 6 (solid curves) yielding the rate constants shown.

(43) For the coordination of simple diazine, HN=NH, see: (a) Albertin, G.; Antoniutti, S.; Bacchi, A.; Boato, M.; Pelizzi, G. *J. Chem. Soc., Dalton Trans.* **2002**, 3313. (b) Smith, M. R.; Cheng, T.-Y.; Hillhouse, G. L. *J. Am. Chem. Soc.* **1993**, *115*, 8638. (c) Cheng, T.-Y.; Peters, J. C.; Hillhouse, G. L. *J. Am. Chem. Soc.* **1994**, *116*, 204.

(44) Que, L., Jr. *J. Chem. Soc., Dalton Trans.* **1997**, 3933.

(45) Brown, S. N.; Mayer, J. M. *Inorg. Chem.* **1992**, *31*, 4091.

(46) Maatta, E. A.; Wentworth, R. A. *Inorg. Chem.* **1980**, *19*, 2597.

(47) KINETIC version 1.04; ARSoftware, 1994.

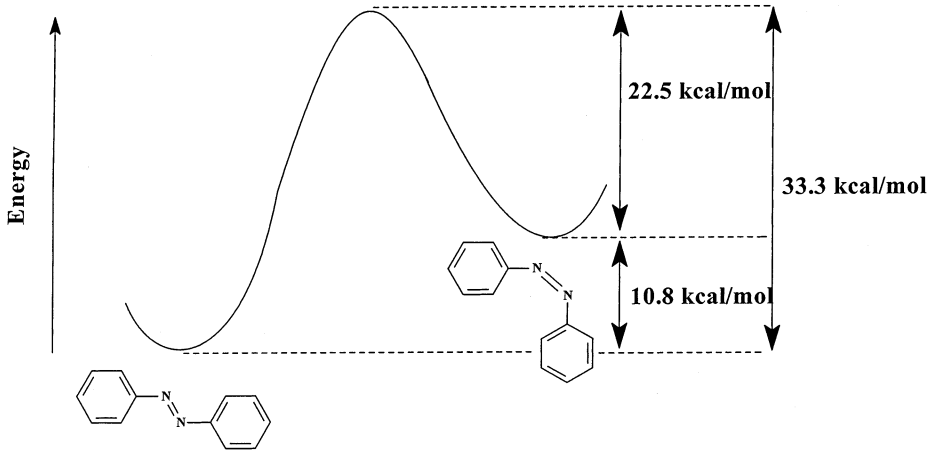

Figure 12. Energy level diagram for *cis*-/*trans*-azobenzene.

comparing it to the low-temperature limiting spectrum of **9** and the chemical shift of free PMe_3. This calculation yielded a value of 9900 M^{-1} L. This is slightly higher than that obtained from the kinetic data, but a significant error will be involved in assuming that the chemical shift of the fully formed complex **9** is invariant with temperature.

The kinetic data, combined with the observed reaction products, clearly show these reactions to occur at a single metal center. However, they do not give us any direct insight into the intimate mechanism of the reaction. Of particular significance is the fact that the kinetic and synthetic studies were carried out using *trans*-azobenzenes. Thermodynamic data show that *trans*-azobenzene is ~10.8 kcal mol^{-1} more stable than the cis isomer.[48] Furthermore, there is a sizable barrier to interconversion (Figure 12). The trans form is ideally suited for the bimolecular activation of the N=N bond via σ-coordination to two different metal centers. However, activation by one metal center eventually requires η^2-coordination (diazametallacyclopropane intermediate). There are many examples in the literature of the formation of η^2-azobenzene complexes directly from *trans*-azobenzene.[41] Recent studies by Bergman et al.[42] show that the reaction of *trans*-azobenzene with the d^2 reagent [Cp_2TaMe] can lead either to terminal imido complexes via cleavage or to the η^2-azobenzene complex. This latter species does not contain the electrons needed to cleave the N=N bond. Hence, it is certain that η^2 coordination can result via reaction with the trans isomer. How this takes place is unknown. It is possible that the barrier to isomerization of σ-bound *trans*-azobenzene is lower than for the free ligand. Alternatively, it is possible that coordination to the π-bond (pseudo-olefin) could lead directly to the η^2-azobenzene intermediate. The cis isomer of azobenzene can be generated photochemically by irradiation of solutions of the trans isomer. Furthermore, it has a lifetime of hours at ambient temperatures. When a photogenerated mixture of *cis*-/*trans*-azobenzene was treated with **4b**, the ratio of cis/trans isomers rapidly dropped with the formation of **8**. This result implies that the cis isomer

Scheme 7

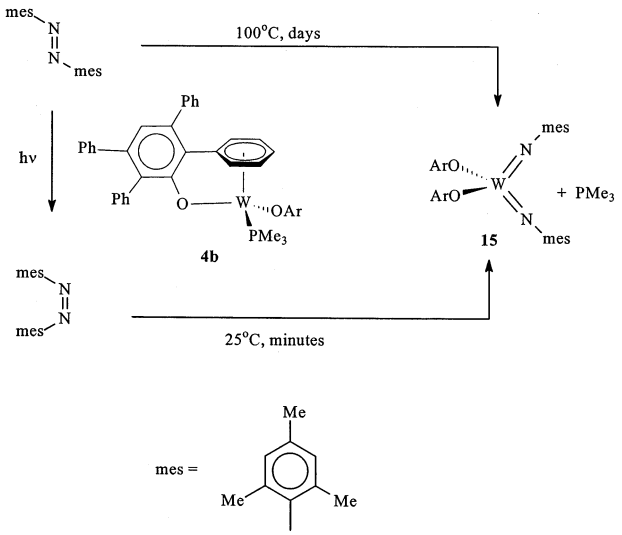

reacts considerably faster than the trans form. This was confirmed by studying the reactivity of bis(2,4,6-trimethylphenyl)diazine, MesN=NMes (NMes = $NC_6H_3Me_3$-2,4,6).[49] Reaction between *trans*-MesN=NMes and **4b** in C_6D_6 solution does not occur over days at room temperature, as monitored by ^1H NMR. Even at 100 °C reaction is slow, needing days to generate a product whose spectroscopic properties are consistent with the formulation [$W(OC_6HPh_4$-2,3,5,6$)_2(NMes)_2$] (**15**) (Scheme 7). Uncoordinated PMe_3 was also observed. When *trans*-MesN=NMes is photolyzed in C_6D_6, the formation of the cis isomer is observed by NMR. Addition of **4b** to this mixture was found to lead to **15** (verified by ^1H NMR) at ambient temperatures within 30 min (Scheme 7). Hence, this is conclusive proof of the much faster reactivity of *cis*-diazines over *trans*-diazines with the W(II) aryloxides **4**. Taken together, the evidence makes a compelling argument that these cleavage reactions (four-electron reductions) are taking place at a single metal center.[50]

Experimental Section

All operations were carried out either under a dry nitrogen atmosphere in a Vacuum Atmospheres Dri-Lab or by standard

(48) (a) Forber, C. L.; Kelusky, E. C.; Bunce, N. J.; Zerner, M. C. *J. Am. Chem. Soc.* **1985**, *107*, 5884. (b) Dias, A. R.; Minas Da Piedade, M. E.; Martinho Simões, J. A.; Simoni, J. A.; Teixeira, C.; Diogo, H. P. *J. Chem. Thermodyn.* **1992**, *24*, 439. (c) Brown, E. V.; Granneman, G. R. *J. Am. Chem. Soc.* **1975**, *97*, 621.

(49) Gabe, E. J.; Wang, Y.; Barclay, L. R. C.; Dust, J. M. *Acta Crystallogr., Sect. B: Struct. Crystallogr., Cryst. Chem.* **1981**, *37*, 978.

(50) Theoretical studies indicate that the final cleavage of the N−N bond in the diazine complex [$(HO)_2W(HNNH)$] occurs during a structural change from pseudo square planar to pseudo tetrahedral.[11]

Schlenk techniques. The hydrocarbon solvents were distilled from sodium benzophenone and stored over sodium ribbon under nitrogen until use. The syntheses of 2,3,5,6-tetraphenylphenol, 2,6-diphenyl-3,5-dimethylphenol, and 2,6-diphenyl-3,5-di-*tert*-butylphenol were previously reported. All phosphines were purchased from Strem Chemical Co. and stored over 4 Å molecular sieves (liquids) or dried under vacuum (solids) for 24 h prior to use. The ^{1}H and ^{13}C NMR spectra (where solubility allowed) were recorded on Varian Associates Gemini-200 and Inova-300 spectrometers and referenced to protio impurities of commercial benzene-d_6. ^{31}P NMR spectra were recorded on a Varian Associates Inova-300 spectrometer and referenced to external 85% H_3PO_4. Elemental analyses and crystallographic studies were obtained in house at Purdue University.

[W(OC$_6$HPh$_4$-2,3,5,6)$_2$Cl$_4$] (1). A 1 L round-bottom flask was charged with [WCl_6] (26.7 g, 0.067 mol) under a nitrogen flush, and 400 mL of toluene was added. With stirring, 2,3,5,6-tetraphenylphenol (53.4 g, 0.14 mol) was added over a 20 min period using a solid addition funnel. Part of the solvent, as well as the HCl gas that was generated, was removed in vacuo and the purple solution refluxed for the next 6 h. The remaining solvent was removed in vacuo to leave the crude product. The purple solid was washed with a small amount of pentane and dried in vacuo to give **1** (75 g, 88%). Anal. Calcd for $C_{60}H_{42}Cl_4O_2W$: C, 64.31; H, 3.78; Cl, 12.65. Found: C, 64.48; H, 3.42; Cl, 12.39. ^{1}H NMR (C_6D_6, 30 °C): δ 7.00−8.00 (m, 42 H, aromatics).

[W(OC$_6$HPh$_2$-2,6-Me$_2$-3,5)$_2$Cl$_4$] (2). To a solution containing [WCl_6] (14.1 g, 0.035 mol) in toluene (200 mL) was added 2,6-diphenyl-3,5-dimethylphenol (20.0 g, 0.073 mol) in portions over a 30 min period. Upon complete addition the dark purple mixture was heated to reflux and vented occasionally to remove HCl from the reaction. The reaction mixture was refluxed for several hours and cooled and the solvent removed in vacuo. The purple solid was washed with a small portion of pentane and dried to give **2** (26.8 g, 89%). Anal. Calcd for $C_{40}H_{34}O_2Cl_4W$: C, 56.88; H, 4.14; Cl, 15.47. Found: C, 56.93; H, 4.14; Cl, 15.56. ^{1}H NMR (C_6D_6, 30 °C): δ 7.0−7.4 (m, 20H, aromatics), 6.34 (s, para *H*), 1.83 (s, CH_3). ^{13}C NMR (C_6D_6, 30 °C): δ 127−140 (aromatics), 20.8 (*C*H$_3$).

[W(OC$_6$HPh$_2$-2,6-Bu$^t_2$-3,5)$_2$Cl$_4$] (3). To a suspension of [WCl_6] (0.54 g, 1.4 mmol) in toluene (100 mL) was added 2 equiv of 3,5-di-*tert*-butyl-2,6-diphenylphenoxide (1.0 g, 2.9 mmol). The solution was stirred for 24 h and filtered, and the solvent was removed under vacuum. The remaining purple powder was recrystallized from toluene layered with hexane as a deep purple powder, giving **3** (0.81 g, 56%). Anal. Calcd for $C_{52}H_{58}Cl_4O_2W$: Cl, 13.63. Found: Cl, 13.24. ^{1}H NMR (C_6D_6, 30 °C): 7.52−7.00 (m, aromatics); 1.12 (s, C(CH_3)$_3$).

[W(OC$_6$HPh$_3$-η^6-C$_6$H$_5$)(OC$_6$HPh$_4$-2,3,5,6)(η^1-dppm)] (4a). A solution of **1** (2.00 g, 1.8 mmol) and dppm (0.69 g, 1.8 mmol) in toluene (25 mL) was stirred over a sodium amalgam (0.20 g of Na, 8.70 mmol) for 48 h at room temperature. The olive green solution was decanted off the mercury pool, filtered through a pad of Celite, and evaporated in vacuo to yield a green solid. The crude solid was recrystallized in a minimum amount of benzene layered with hexane, giving **4d** (1.8 g, 25%) as green crystals. Anal. Calcd for $C_{85}H_{64}O_2PW$: C, 74.90; H, 4.72; P, 4.51. Found: C, 74.56; H, 4.73; P, 4.18. ^{1}H NMR (C_6D_6, 30 °C): δ 6.8−7.7 (m, 37 H, aromatic protons), 4.44, 3.16, 2.07, 1.82, 1.79 (m, η^6-C$_6$H$_5$), 3.19, 2.55 (multiplet, diastereotopic methylene protons of dppm). ^{31}P NMR (C_6D_6, 30 °C): δ 52.9 (d, $^2J(^{31}P-^{31}P)$ = 45.3 Hz, $^1J(^{183}W-^{31}P)$ = 358 Hz), −24.9 (d).

[W(OC$_6$HPh$_3$-η^6-C$_6$H$_5$)(OC$_6$HPh$_4$-2,3,5,6)(PMe$_3$)] (4b). A solution of **1** (4.00 g, 3.6 mmol) and an excess (2.2−2.5 equiv per W) of PMe_3 in toluene (50 mL) was stirred over a sodium amalgam (0.40 g of Na, 17.4 mmol) for 24 h at room temperature. The resulting olive green solution was decanted off the mercury pool, filtered through a pad of Celite, and evaporated in vacuo to yield a green solid. The crude solid was recrystallized in a minimum amount of benzene layered with hexane, giving **4a** (1.5 g, 40%) as crystals suitable for an X-ray diffraction study. Anal. Calcd for $C_{63}H_{52}PO_2W$: C, 71.66; H, 4.96; P, 2.93. Found: C, 71.83; H, 5.02; P, 2.83. For ^{1}H NMR data at −30 °C in toluene-d_8 see Table 2. ^{1}H NMR (C_6D_6, 30 °C): δ 7.00−8.00, 3.45, 2.94, 1.94, 1.52, 1.19 (m, η^6-C$_6$H$_5$), 0.96 (d, PMe_3). ^{13}C NMR (C_6D_6, 30 °C): δ 169.7, 165.9, 143.1, 141.4, 141.3, 140.2, 139.4, 138.4, 137.2, 132.9, 132.3, 130.5, 130.2, 129.9, 129.3, 129.0, 128.5, 128.1, 127.8, 127.0, 126.3, 125.7, 124.6, 120.0 (aromatic *C*), 100.6, 96.2, 94.0, 92.0 (br, η^6-C$_6$H$_5$), 16.0 (d, PMe_3). ^{31}P NMR (C_6D_6, 30 °C): δ 31.6 ($^1J(^{183}W-^{31}P)$ = 372 Hz).

[W(OC$_6$HPh$_3$-η^6-C$_6$H$_5$)(OC$_6$HPh$_4$-2,3,5,6)(PEt$_3$)] (4c). A solution of **1** (4.06 g, 3.63 mmol) and PEt_3 (1.33 mL, 9.0 mmol) in toluene (100 mL) was stirred over a sodium amalgam (0.40 g of Na, 17.4 mmol) for 24 h at room temperature. The olive green solution was decanted off the mercury pool, filtered through Celite, and evaporated in vacuo to yield a dark green solid. The crude solid was recrystallized in a minimal amount of toluene layered with pentanes, giving **4c** (1.82 g, 45.8%) as emerald green crystals suitable for an X-ray diffraction study. Anal. Calcd for $C_{66}H_{57}O_2PW$: C, 72.26; H, 5.24; P, 2.82. Found: C, 72.55; H, 5.42; P, 2.65. ^{1}H NMR (d_6-benzene, 25 °C): δ 7.72 (d, 2H, aromatic), 7.72−6.88 (m, aromatics), 3.65 (broad m, 1H, *m*-η^6-arene), 2.99 (broad m, 1H, *o*-η^6-arene), 1.83 (broad m, 1H, *m*-η^6-arene), 1.57 (broad m, 1H, *o*-η^6-arene), 1.28 (m, 7H, *p*-η^6-arene and P−CH_2CH$_3$), 0.57 (m, 9H, P−CH$_2$CH_3). ^{13}C NMR (C_6D_6, 20° C): δ 142.7, 141.3, 141.2, 138.5, 132.3, 130.3, 129.9, 129.7, 129.0, 128.7, 128.4, 128.3, 126.8, 126.3, 126.0, 125.6, 125.5, 125.4, 124.3, 119.8 (aromatic *C*), 16.3 (d, P−*C*H$_2$−), 7.4 (−*C*H$_3$). ^{31}P NMR (C_6D_6, 20° C): δ 59.0 ($^1J(^{183}W-^{31}P)$ = 363 Hz).

[W(OC$_6$HPh$_3$-η^6-C$_6$H$_5$)(OC$_6$HPh$_4$-2,3,5,6)(PBu$^n_3$)] (4d). A solution of **1** (2.00 g, 1.8 mmol) and PBu$^n_3$ (0.40 g, 1.8 mmol) in toluene (25 mL) was stirred over a sodium amalgam (0.20 g of Na, 8.70 mmol) for 24 h at room temperature. The olive green solution was decanted off the mercury pool, filtered through a pad of Celite, and evaporated in vacuo to yield a green solid. The crude solid was recrystallized in a minimum amount of benzene layered with hexane, giving **4e** (0.55 g, 25%) as a green powder. Anal. Calcd for $C_{72}H_{69}O_2PW$: C, 73.22; H, 5.89; P, 2.62. Found: C, 73.46; H, 6.22; P, 2.31. ^{1}H NMR (C_6D_6, 30 °C): δ 6.8−7.7 (m, 37 H, aromatic protons), 3.76 (q, 1 H), 3.03 (t, 1 H), 1.86 (q, 1 H), 1.71 (d, 1 H, η^6-C$_6$H$_5$), 1.5 (m), 1.2 (m), 0.9 (m, PBu_3). ^{13}C NMR (C_6D_6, 30 °C): δ 179.2 (d), 165.2 (d), 143.4, 143.0, 142.2, 141.5, 139.8, 139.6, 139.2, 138.5, 137.4, 132.6, 131.0, 130.6, 129.5, 129.2, 129.0, 127.0, 126.8, 126.2, 125.6, 120.2 (aromatic *C*), 99.4, 98.7, 98.4, 97.0, 96.8, 93.2 (η^6-C$_6$H$_5$), 25.8, 24.7, 24.6 (d), 14.2 (PBu_3). ^{31}P NMR (C_6D_6, 30 °C): δ 52.9 ($^1J(^{183}W-^{31}P)$ = 364 Hz).

[W(OC$_6$HPh$_3$-η^6-C$_6$H$_5$)(OC$_6$HPh$_4$-2,3,5,6)(PMe$_2$Ph)] (4e). A solution of **1** (2.00 g, 1.8 mmol) and PMe_2Ph (0.25 g, 1.8 mmol) in toluene (25 mL) was stirred over a sodium amalgam (0.20 g of Na, 8.70 mmol) for 48 h at room temperature. The olive green solution was decanted off the mercury pool, filtered through a pad of Celite, and evaporated in vacuo to yield a green solid. The crude solid was recrystallized in a minimum amount of benzene layered with hexane, giving **4b** (0.75 g, 40%) as emerald green crystals suitable for an X-ray diffraction study. Anal. Calcd for $C_{68}H_{53}O_2PW$: C, 73.10; H, 4.83; P, 2.83. Found: C, 72.78; H, 4.92; P, 2.49. ^{1}H NMR (C_6D_6, 30 °C): δ 6.8−7.8 (m, 37 H, aromatic protons), 3.50, 3.04, 2.02, 1.70, 1.38 (m, η^6-C$_6$*H*$_5$), 1.22 (d, PMe_2Ph); 1.13 (d, PMe_2Ph). ^{13}C NMR (C_6D_6, 30 °C): δ 177.5 (d), 165.5 (d), 142.9, 142.3, 141.6, 141.4, 141.2, 140.6, 140.1, 139.6, 139.2, 138.7, 137.0, 132.7, 132.3, 131.4, 131.2, 130.5, 130.1 129.3, 129.0, 128.3, 127.7, 126.9, 126.6, 126.3, 125.9, 124.5, 119.9 (aromatic *C*); 100.2, 97.6, 95.5, 92.2 (br, η^6-C$_6$H$_5$), 15.5 (d, PMe_2Ph), 14.4 (d, PMe_2Ph). ^{31}P NMR (C_6D_6, 30 °C): δ 38.1 ($^1J(^{183}W-^{31}P)$ = 367 Hz).

[W(OC$_6$HPh$_3$-η^6-C$_6$H$_5$)(OC$_6$HPh$_4$-2,3,5,6)(PMePh$_2$)] (4f). A solution of **1** (2.00 g, 1.8 mmol) and $PMePh_2$ (0.40 g, 1.8

mmol) in toluene (25 mL) was stirred over a sodium amalgam (0.20 g of Na, 8.70 mmol) for 24 h at room temperature. The olive green solution was decanted off the mercury pool, filtered through a pad of Celite, and evaporated in vacuo to yield a green solid. The crude solid was recrystallized in a minimum amount of benzene layered with hexane, giving **4c** (0.55 g, 25%) as green crystals. ^{1}H NMR (C_6D_6, 30 °C): δ 6.8−7.7 (m, 37 H, aromatic protons), 3.66, 3.12, 2.04, 1.48 (m, η^6-C_6H_5), 1.26 (d, P−*Me*). ^{13}C NMR (C_6D_6, 30 °C): δ 178.4 (d), 165.7 (d), 143.0, 141.6, 141.4, 140.2, 139.7, 139.3, 138.0, 137.2, 133.7, 132.8, 130.5, 130.0, 129.6, 129.3, 127.0, 126.7, 126.3, 126.2, 125.5, 124.7, 120.3 (aromatic *C*), 99.9, 99.8, 99.1, 98.2, 93.3, 93.0 (η^6-C_6H_5), 15.8 (d, $PMePh_2$). ^{31}P NMR (C_6D_6, 30 °C): δ 49.1 ($^1J(^{183}W-^{31}P)$ = 362 Hz).

[W(OC$_6$HPh-η^6-C$_6$H$_5$-Me$_2$-3,5)(OC$_6$HPh$_2$-2,6-Me$_2$-3,5)(η^1-dppm)] (5a). A solution of **2** (1.30 g, 1.5 mmol) and dppm (0.65 g, 1.65 mmol) in toluene (25 mL) was stirred over a sodium amalgam (0.16 g of Na, 6.7 mmol) for 3 h at room temperature. The solution was decanted off the mercury pool, filtered through a Celite pad, and evaporated in vacuo to yield **5** as a deep green solid. Anal. Calcd for $C_{65}H_{56}O_2P_2W$: C, 71.90; H, 5.16. Found: C, 71.80; H, 5.32. ^{1}H NMR (C_6D_6, 30 °C): δ 6.6−7.6 (m, aromatic *H*), 6.57 (s, *p*-*H*), 6.46 (s, *p*-*H*), 4.34, 3.36, 3.07, 2.47, 1.73 (m, η^6-C_6H_5), 2.72 (m, dppm). ^{13}C NMR (C_6D_6, 30 °C): δ 177.6 (d, W−O−*C*, $^3J(^{31}P-^{13}C)$ = 10.1 Hz), 164.9 (d, W−O−*C*, $^3J(^{31}P-^{13}C)$ = 5.6 Hz), 139.0, 135.3, 134.8, 133.9, 133.7, 133.6, 133.5, 133.3 133.2, 133.0, 132.9, 132.7, 132.6, 132.5, 131.8, 129.2, 127.8, 127.3, 126.5, 125.6, 124.1 (d, $^1J(^{31}P-^{13}C)$ = 5.5 Hz), 99.1, 98.9, 98.8, 98.6, 92.6, 92.4 (η^6-*C*$_6$H$_5$), 26.6 (m, dppm), 24.6, 20.6, 19.2 (*m*-Me). ^{31}P NMR (C_6D_6, 30 °C): δ 57.0 (d, $^2J(^{31}P-^{31}P)$ = 56.3 Hz, $^1J(^{183}W-^{31}P)$ = 357 Hz), −24.73 (d, $^2J(^{31}P-^{31}P)$ = 56.3 Hz).

Preparation of [W(OC$_6$HPh-η^6-C$_6$H$_5$-Bu$^t_2$-3,5)(OC$_6$HPh$_2$-2,6-Bu$^t_2$-3,5)(η^1-dppm)] (6a). A solution of **3** (0.30 g, 0.3 mmol) and dppm (0.20 g, 0.5 mmol) in 15 mL of toluene was stirred over a sodium amalgam (0.03 g of Na, 1.3 mmol) for 3 h at room temperature. The solution was decanted off the mercury pool, filtered through a Celite pad, and evaporated in vacuo to yield **6a** (0.31 g, 80%) as a deep green solid. ^{1}H NMR (C_6D_6, 30 °C): δ 6.5−7.8 (m, aromatics), 3.93, 2.75, 2.5, 2.35 (m, protons of the η^6-C_6H_5 group and methylene protons from dppm), 1.31 (s, C(C*H*$_3$)$_3$), 1.12, 1.25 (s, inequivalent C(C*H*$_3$)$_3$ from η^6-bound aryloxide). ^{13}C NMR (C_6D_6, 30 °C): δ 180.2 (W−O−*C* from η^6-bound aryloxide), 167.5 (W−O−*C*), 147.3, 147.1, 140.8, 139.6, 137.7, 133.2, 131.9, 129.5, 129.3, 127.9, 127.5, 127.0, 126.4, 126.0, 125.8, 125.6, 125.5 (aromatics), 101.8, 99.9, 98.0, 91.7 (η^6-*C*$_6$H$_5$), 37.4, 37.3, 36.6 (*C*(CH$_3$)$_3$), 33.8, 33.7, 33.1 (C(*C*H$_3$)$_3$). ^{31}P NMR (C_6D_6, 30 °C): δ 58.3 (unresolved doublet with ^{183}W satellites, $^1J(^{183}W-^{31}P)$ = 342 Hz), −24.1 (d, $^2J(^{31}P-^{31}P)$ = 32.2 Hz).

Preparation of [W(OC$_6$HPh$_4$-2,3,5,6)$_2$(O)$_2$(PMe$_3$)] (7). A saturated C_6D_6 solution of [W(OC$_6$HPh$_3$-η^6-C$_6$H$_5$)(OC$_6$HPh$_4$-2,3,5,6)(η^1-PMe$_3$)] in a 5 mm J. Young NMR tube was degassed and placed under an atmosphere of pure oxygen. The emerald green solution faded to yellow brown within minutes. Layering the solution with hexane induced the formation of yellow crystals that were suitable for an X-ray diffraction study. Anal. Calcd for $C_{63}H_{51}PO_2W{\cdot}C_6H_6$: C, 71.14; H, 4.93. Found: C, 71.52; H, 4.79. ^{1}H NMR (30 °C, C_6D_6): δ 6.8−7.5 (aromatics), 0.18 (d, PMe_3). ^{31}P NMR (30 °C, C_6D_6): δ −2.5 (br, *P*Me$_3$).

Preparation of [W(OC$_6$HPh$_4$-2,3,5,6)$_2$(NPh)$_2$(PMe$_3$)] (8). A saturated C_6D_6 solution of [W(OC$_6$HPh$_3$-η^6-C$_6$H$_5$)(OC$_6$HPh$_4$-2,3,5,6)(PMe$_3$)] was treated with an excess of azobenzene, and the emerald green solution quickly turned orange-brown. After several hours the product was analyzed using NMR spectroscopy. ^{1}H NMR (C_6D_6, 30 °C): δ 6.8−7.5 (aromatics), 6.63 (t, *p*-H of NPh); 6.59 (d, *o*-H of NPh). ^{31}P NMR (C_6D_6, 30 °C): δ 0.30 ppm (br, *P*Me$_3$).

Preparation of [W(OC$_6$HPh$_4$-2,3,5,6)$_2$(NTol)$_2$(PMe$_3$)] (9). A saturated C_6D_6 solution of [W(OC$_6$HPh$_3$-η^6-C$_6$H$_5$)(OC$_6$HPh$_4$-2,3,5,6)(PMe$_3$)] was treated with an excess of TolN═NTol, and the emerald green solution quickly turned orange-brown; after several hours the product was analyzed using NMR spectroscopy. ^{1}H NMR (C_6D_6, 30 °C): δ 6.9−7.5 (aromatics), 6.82 (d, 8.30 Hz, *m*-H), 6.51 (d, 8.05 Hz, *o*-H), 2.12 (s, *p*-Me), 0.10 (br, PMe_3). ^{31}P NMR (C_6D_6, 30 °C): δ 4.1 ppm (br, *P*Me$_3$).

Preparation of [W(OC$_6$HPh$_4$-2,3,5,6)$_2$(NPh)(NTol)(PMe$_3$)] (10). A saturated C_6D_6 solution of [W(OC$_6$HPh$_3$-η^6-C$_6$H$_5$)(OC$_6$HPh$_4$-2,3,5,6)(PMe$_3$)] was treated with an excess of TolN═NPh, and the emerald green solution quickly turned orange-brown. Layering the solution with hexanes induced the formation of crystals that were suitable for an X-ray diffraction study. ^{1}H NMR (C_6D_6, 30 °C): δ 6.94−8.03 (aromatics), 6.80 (d, 8.06 Hz, *m*-H of NTol), 6.66 (t, 7.45 Hz, *p*-H of NPh), 6.59 (d, 8.01 Hz, *o*-H of NPh), 6.67 (d, 8.06 Hz, *o*-H of NTol), 2.11 (s, 3H, *p*-Me), 0.26 (br, PMe_3). ^{31}P NMR (C_6D_6, 30 °C): δ 3.0 ppm (br, *P*Me$_3$).

Preparation of [W(OC$_6$HPh$_4$-2,3,5,6)$_2$(NPh)(O)(OPMe$_3$)] (11). A saturated C_6D_6 solution of [W(OC$_6$HPh$_3$-η^6-C$_6$H$_5$)(OC$_6$HPh$_4$-2,3,5,6)(PMe$_3$)] was treated with an excess of nitrosobenzene, and the emerald green solution quickly turned brown. Layering the solution with hexanes induced the formation of crystals that were suitable for an X-ray diffraction study. ^{1}H NMR (C_6D_6, 30 °C): δ 6.5−7.9 (aromatics), 6.74 (t, *p*-H of NPh), 6.19 (d, *o*-H of NPh), 0.58 (br, OPMe$_3$). ^{31}P NMR (C_6D_6, 30 °C): δ 32.7 ppm (br, O*P*Me$_3$).

Preparation of [W(OC$_6$HPh$_4$-2,3,5,6)$_2$(NC$_4$H$_4$N)(PMe$_3$)] (12). A sample of **4b** (97.4 mg, mmol) was dissolved in 1 mL of d_6-benzene, and to this solution was added 1 equiv of pyridazine (6.7 μL, mmol). Upon addition the solution went from emerald green to red. The sample was analyzed by NMR spectroscopy. **12** was recrystallized in hot benzene, and red crystals suitable for an X-ray diffraction study formed. Anal. Calcd for $C_{67}H_{55}N_2O_2W$: C, 70.90; H, 4.88; N, 2.47; P, 2.73. Found: C, 69.89; H, 4.91; N, 2.12; P, 2.38. ^{1}H NMR (C_6D_6, 25 °C): δ 7.6 (dd, *H*C−N), 7.3−6.9 (m, aromatics), 5.8 (dd, 2H, *H*C═C*H*), −0.24 (d, P*Me*$_3$). ^{31}P NMR (C_6D_6, 25 °C): δ −11 (br, PMe_3).

Preparation of [W(OC$_6$HPh$_4$-2,3,5,6)$_2$(NC$_{12}$H$_8$N)(PMe$_3$)] (13). A sample of **4b** (100 mg, 0.095 mmol) was dissolved in 4 mL of benzene, and to this solution was added an excess of benzo[*c*]cinnoline (35 mg, 0.20 mmol). The solution was stirred for 2 h at room temperature. Afterward, the solution was layered with hexanes and the yellow precipitate was dried in vacuo (65 mg, 55.6%). The product was analyzed by NMR spectroscopy. Yellow-green X-ray-quality crystals were obtained by dissolving the crude product in a minimum amount of benzene and layering the solution with hexane. Anal. Calcd for $C_{75}H_{59}N_2O_2PW$: C, 72.93; H, 4.82; N, 2.27. Found: C, 73.11; H, 5.02; N, 2.38. ^{1}H NMR (C_6D_6, 25 °C): δ 6.94−7.5 (m, aromatics), 7.6 (d, *o*-H), 6.8 (t, *p*-H), 6.6 (d, *m*-H), −0.09 (d, PMe_3). ^{31}P NMR (C_6D_6, −50 °C): δ −0.477 ($^1J(^{183}W-^{31}P)$ = 338 Hz).

Preparation of [W(OC$_6$HPh$_4$-2,3,5,6)$_2${NCH(C$_6$H$_4$)CHN}(PMe$_3$)] (14). A sample of **4b** (150 mg, 0.142 mmol) was dissolved in 4 mL of benzene, and to this solution was added phthalazine (19 mg, 0.146 mmol). The solution was stirred for 20 min at room temperature and then layered with hexanes, giving dark green crystals of **14** (85.7 mg, 50.9%) suitable for X-ray diffraction study (0.0857 g, 50.9%). Anal. Calcd for $C_{71}H_{57}N_2O_2PW$: C, 71.96; H, 4.85; N, 2.36; P, 2.61. Found: C, 72.41; H, 5.07; N, 2.38; P, 2.50. ^{1}H NMR (C_6D_6, 25 °C): δ 8.5 (s, *o*-H to N), 7.0−7.4 (m, aromatics), 7.2 (dd, aromatics), −0.5 (d, PMe_3). ^{31}P NMR (toluene-d_8, −30 °C): δ −17.58 ($^1J(^{183}W-^{31}P)$ = 296 Hz).

Preparation of [W(OC$_6$HPh$_4$-2,3,5,6)$_2$(NMes)$_2$] (15). A sample of **4b** (81.6 mg, 0.077 mmol) was placed in a J. Young valve solvent seal NMR tube along with d_6-benzene (1 mL). To this solution was added an excess of *trans*-azomesitylene (25.8 mg, 0.097 mmol). The solution was photolyzed for 20 min using a mercury−tungsten lamp and then heated for 5 min at 100 °C. Yield: 0.0752 g (78%). Anal. Calcd for $C_{78}H_{64}N_2O_2W$: C, 75.23; H, 5.18; N, 2.26. Found: C, 74.85; H,

Table 9. Crystal Data and Data Collection Parameters

	4b	4c	4d	7	10	11	12	13	14
formula	$WPO_2C_{63}H_{56}$	$WPO_2C_{66}H_{57}\cdot C_6H_6$	$WPO_2C_{72}H_{69}$	$WPO_4C_{63}H_{51}\cdot C_6H_6$	$WPO_2N_2C_{76}H_{63}$	$WPO_4NC_{69}H_{56}\cdot C_6H_6$	$WPO_2N_2C_{67}H_{55}\cdot 2C_6H_6$	$WPO_2N_2C_{75}H_{59}\cdot 2C_6H_6$	$WPO_2N_2C_{71}H_{57}$
fw	1059.97	1175.13	1181.18	1165.05	1251.19	1256.16	1291.25	1391.37	1185.08
space group	$P\bar{1}$ (No. 2)	$P2_1/c$ (No. 14)	$P\bar{1}$ (No. 2)	$P2_1/n$ (No. 14)	$P2_1/n$ (No. 14)	$P2_1/n$ (No. 14)	$P2_1/c$ (No. 14)	$P2_1/c$ (No. 14)	$P\bar{1}$ (No. 2)
a, Å	11.5631(3)	10.7808(2)	11.620(3)	12.4708(2)	11.4420(3)	14.5298(4)	24.8331(5)	12.2150(2)	11.3255(1)
b, Å	12.3496(2)	23.9094(9)	14.612(3)	14.9833(2)	27.6755(7)	17.7437(5)	11.5704(3)	32.4594(5)	16.3547(3)
c, Å	18.2185(4)	22.8885(8)	18.953(2)	30.1291(5)	19.8378(4)	23.2712(6)	44.5364(12)	17.0957(2)	18.3239(3)
α, deg	82.6659(16)	90	102.809(12)	90	90	90	90	90	70.6136(7)
β, deg	72.7035(11)	90.541(2)	91.441(15)	98.1813(8)	104.9040(13)	97.4297(17)	101.3130(8)	93.0186(9)	73.1055(6)
γ, deg	86.8764(16)	90	109.153(17)	90	90	90	90	90	71.103(1)
V, Å	2463.25(13)	5899.5(5)	2947	5572.4(3)	6070.6(5)	5997.7(5)	12548.0(10)	6768.9(3)	2964.6(1)
Z	2	4	2	4	4	4	8	4	2
ρ_{calcd}, g cm^{-3}	1.429	1.323	1.331	1.389	1.369	1.391	1.367	1.365	1.327
temp, K	203.	150.	296.	203.	203.	203.	150.	150.	150.
radiation (λ)	Mo Kα (0.710 73 Å)								
R	0.042	0.050	0.040	0.051	0.044	0.048	0.051	0.042	0.038
R_w	0.111	0.115	0.042	0.106	0.098	0.092	0.084	0.089	0.085

5.33; N, 2.12. ^{1}H NMR (C_6D_6, 25 °C): δ 6.8−7.3 (m, aromatics) 6.69 (s, *m*-H on NMes), 2.15 (s, *o*-Me on mesitylene), 1.86 (s, *p*-Me on mesitylene).

X-ray Data Collection and Reduction. Crystal data and data collection parameters are contained in Table 9. A suitable crystal was mounted on a glass fiber in a random orientation under a cold stream of dry nitrogen. Preliminary examination and final data collection were performed with Mo Kα radiation (λ = 0.710 73 Å) on a Nonius Kappa CCD diffractometer. Lorentz and polarization corrections were applied to the data.[51] An empirical absorption correction using SCALEPACK was applied.[52] Intensities of equivalent reflections were averaged. The structure was solved using the structure solution program PATTY in DIRDIF92.[53] The remaining atoms were located in succeeding difference Fourier syntheses. Hydrogen atoms were included in the refinement but restrained to ride on the atom to which they are bonded. The structure was refined in full-matrix least squares, where the function minimized was $\sum w(|F_o|^2 - |F_c|^2)^2$ and the weight w is defined as $w = 1/[\sigma^2(F_o^2) + (0.0585P)^2 + 1.4064P]$, where $P = (F_o^2 + 2F_c^2)/3$. Scattering factors were taken from ref 54. Refinement was performed on a AlphaServer 2100 using SHELX-97.[55] Crystallographic drawings were done using the ORTEP program.[56]

Acknowledgment. We thank the National Science Foundation (Grant No. CHE-0078405) for financial support of this research. We thank Prof. Greg Hillhouse for a generous sample of *trans*-azomesitylene. We thank Drs. Klaas Halenga and Edwin Rivera for all their helpful NMR advice and instruction.

Supporting Information Available: Tables giving X-ray crystallographic data for **4b**−**d**, **7**, and **10**−**14**. This material is available free of charge via the Internet at http://pubs.acs.org.

OM030604M

(51) McArdle, P. C. *J. Appl. Crystallogr.* **1996**, *239*, 306.
(52) Otwinowski, Z.; Minor, W. *Methods Enzymol.* **1996**, 276.
(53) Beurskens, P. T.; Admirall, G.; Beurskens, G.; Bosman, W. P.; Garcia-Granda, R. S.; Gould, O.; Smits, J. M. M.; Smykalla, C. The DIRDIF92 Program System; Technical Report; Crystallography Laboratory, University of Nijmegen, Nijmegen, The Netherlands, 1992.
(54) *International Tables for Crystallography*; Kluwer Academic: Dordrecht, The Netherlands, 1992; Vol. C, Tables 4.2.6.8 and 6.1.1.4.
(55) Sheldrick, G. M. SHELXS97, A Program for Crystal Structure Refinement; University of Gottingen, Gottingen, Germany, 1997.
(56) Johnson, C. K. ORTEPII; Report ORNL-5138; Oak Ridge National Laboratory, Oak Ridge, TN, 1976.